3-11-2011

Modeling of Bacillus Spores: Inactivation and Outgrowth

Alexis X. Hurst

MODELING OF *BACILLUS* SPORES: INACTIVATION AND OUTGROWTH

THESIS

Alexis X. Hurst

AFIT/GAM/ENC/11-01

DEPARTMENT OF THE AIR FORCE
AIR UNIVERSITY

AIR FORCE INSTITUTE OF TECHNOLOGY

Wright-Patterson Air Force Base, Ohio

AFIT/GAM/ENC/11-01

MODELING OF *BACILLUS* SPORES: INACTIVATION AND OUTGROWTH

THESIS

Presented to the Faculty

Department of Mathematics and Statistics

Graduate School of Engineering and Management

Air Force Institute of Technology

Air University

Air Education and Training Command

In Partial Fulfillment of the Requirements for the

Degree of Master of Science in Applied Mathematics

Alexis X. Hurst, BS

March 2011

APPROVED FOR PUBLIC RELEASE; DISTRIBUTION UNLIMITED

AFIT/GAM/ENC/11-01

MODELING OF *BACILLUS* SPORES: INACTIVATION AND OUTGROWTH

Alexis X. Hurst, BS

Approved:

_____	_____
Dr. William P. Baker (Chairman)	Date
_____	_____
Dr. Larry W. Burggraf (Member)	Date
_____	_____
Dr. Christine M. Schubert Kabban (Member)	Date

Abstract

This research models and analyzes the thermochemical damage produced in *Bacillus* spores by short, high-temperature exposures as well the repair process within damaged *Bacillus* spores. Thermochemical damage in spores is significantly due to reaction with water, hydrolysis reactions. Applying heat to the spore causes absorbed and chemically bound water molecules become mobile within the spore. These mobile water molecules react by hydrolysis reactions to degrade DNA and enzyme molecules in the spore. In order to survive the thermal inactivation, the spore must repair the damaged DNA during spore germination. The DNA repair process, as well as other germination functions, is dependent on reactions catalyzed by enzymes that are viable after the thermal exposure. Increased damage to the enzymes during thermal inactivation, affects the rate at which the spore DNA is repaired. If the enzymes are damaged to such an extent that the DNA repair is not completed, the spore is unable to germinate, or produce outgrowth. The DNA repair process, repair enzymes, and outgrowth time influences the spore's chance of survival. Using this information, a probability of survival model was created based on water mobility, hydrolysis reactions, an initial state of DNA, viable repair enzymes, and an outgrowth time.

Acknowledgments

I would like to thank my committee, Dr. Baker, Dr. Burggraf, and Dr. Schubert Kabban, for their support and guidance. I would also like to thank the faculty and staff for helping me along this journey. This has been a very fulfilling opportunity to grow and learn more about the world of applied mathematics.

Alexis X. Hurst

Table of Contents

List of Figures

Page

List of Tables

Page

MODELING OF *BACILLUS* SPORES: INACTIVATION AND OUTGROWTH

1. Introduction

1.1 Background

Anthrax is a bacterial infection that has a high fatality rate of 89% in the United States that occurs when *Bacillus anthracis* (*B.a)* endospores are inhaled into lung alveoli and germinate [4, 18]. Anthrax spores can be easily prepared from *B.a* obtained from infected animals or soil [27]. The spores can be aerosolized and used with intent to harm by causing anthrax disease in humans. The early diagnosis of inhalational anthrax is very difficult, if there no knowledge of the anthrax exposure. Antibiotic treatment is effective only during the first stage of this infection, which is characterized by nonspecific flu-like symptoms. This stage normally lasts for several days. This is followed by the final stage, death sometimes occurs after only a few hours [18]. These are reasons why *B.a* is listed as a biological warfare agent.

Several incidents have occurred involving the agent [26]. In 1979, anthrax spores were accidently released in Sverdlovsk, Russia. The release caused an epidemic of inhalational anthrax in Russia resulting in 66 deaths and 18 cases of exposure to anthrax in the United States. In 1993, Aum Shinrikyo, a Japanese cult, aerosolized a liquid suspension of *B.a* from the roof of an eight story building. The liquid apparently had a low concentration of spores and was ineffective since the *B.a* strain was used to vaccinate animals in Japan. In 2001, anthrax spores were mailed through the United States Postal

Service to members of the U.S. Senate and to national news agencies. These attacks resulted in 22 combined inhalational and cutaneous cases of anthrax infection. Of the 22 cases, five Americans died of inhalational anthrax. These attacks pointed out the possibilities and vulnerabilities of bioterrorism using *B.a*. Furthermore, these attacks illustrated the need for detection, recognition, environmental surveillance, decontamination, and destruction of anthrax.

1.2 Previous Research

Much previous work has been done studying and modeling *B.a*. Researchers at the Air Force Institute of Technology (AFIT) have been researching and developing methods to characterize the effects of heating *B.a* spores at high temperatures for short durations. A previous researcher, Captain Emily Knight [19], has developed a thermal model to predict the effects of the thermal damage to the spores. The thermal model was designed to replicate the laboratory experiments which heat spores at nearly constant temperature for short times. The thermal model evaluates the rate of thermal diffusion throughout the *B.a* spores as well as characterizes the influence that heating has on distributing water within the spore. A water mobility model based on the production-diffusion of water throughout the spore was developed to achieve this goal. Using the water mobility model, Captain Knight presented a probability of kill model that relates repair of the degradation of initial DNA information content to the decimation of the spore population's protein 'fitness'. This model was based on an assumed Gaussian representation of protein fitness distribution.

1.3 Purpose

The purpose for this research is to develop a probability of survival model for *B.a* spores exposed to high temperatures at short exposure times. This research will estimate the concentration of water within the *B.a* spore and the temperatures at which this water will become available for hydrolysis reactions to occur. Hydrolysis is the reaction of molecules with water molecules. Water can react with biopolymers which are molecules such as DNA and proteins resulting in deploymerization (breaking a large strand of polymers into two smaller ones) or denaturation (when proteins or DNA loses their unique three-dimensional structures). This research will use as an input to the water mobility model mathematical fits of measured data of water evolved from *B.a* spores obtained from thermogravimetric analysis conducted by Dr. Daniel Felker.

Hydrolysis reactions can damage the spore's DNA and proteins to such an extent that the DNA cannot be repaired. The extent to which the DNA and proteins have been damaged beyond repair is the critical threshold. The threshold for the enzyme damage influences the threshold for the DNA. This is because the DNA repair process is mediated by the concentration of viable enzymes (proteins that catalyze specific chemical reactions). Therefore, the probability of kill model developed by Captain Knight [19] will be reviewed as well as different representations for the distribution of enzyme fitness.

The spore exist in a dormant state where metabolic activity has stopped and the DNA is immobilized in the spore's core contributing to increase the spore's resistance to damage. The spore can stay in this dormant state for long periods. Once placed in a moist and nutrient-rich environment, the spore will break its dormancy and begin germination. During germination, the spore will repair damaged DNA. The rate of this

repair process depends on the concentration of viable enzymes. Quantitative models by Sokhansanj et al [36] exist for the base excision repair process. These models will be mimicked to obtain a qualitative look at the spore's DNA repair process. Since the enzymes are also damaged during thermal exposure, the DNA repair time will be affected by their damage. If there is little damage to the enzymes, then the repair time will be quicker. Whereas, if there is substantial damage to the enzymes, the repair time would take longer or if the enzyme damage is irreversible the spore cannot repair the damaged DNA. For example, elimination of multiple bases (adenine, guanine, cytosine, thymine) on a single strand of the DNA double helix can be readily, faithfully repaired, but completely cleaving the DNA double helix in multiple locations may not be faithfully repaired. Thus, a spore suffering significant unrepaired DNA damage will not be able to produce outgrowth and, unable to replicate itself, it is permanently inactive, i.e. dead for the purpose of producing disease.

Many parameters influence the repair process. These influences include the initial state of the spore DNA and the concentration of viable enzymes. The concentration of viable enzymes is dependent on the exposure temperature and exposure time.

This research will examine the different influences of these parameters on the repair process and model their effect on the spore's chances of survival. Previously, the probability of kill model was based on an arbitrary estimate of the enzymes' critical threshold. Unfortunately, information about this critical threshold is unknown for *Bacillus* spores. Therefore, this research will develop a probability of kill model based on thermal exposure as well as different combinations of enzymes available for DNA repair process and several outgrowth times. Let outgrowth time be defined as the amount of

time selected to see if the spore produces a viable, replicating cell during germination. Therefore, shorter outgrowth measurement time will lead to a higher measured probability of kill and a longer measured outgrowth time will lead to a shorter measured probability of kill. The actual probability of kill is estimated by very long measurement times. However, there are practicable limits to extending these measurement times. Producing a model of kill probability that includes damage repair necessary for outgrowth will further enhance experimentalists' ability to interpret their data.

1.4 Modeling Objectives

- Analyze thermogravimetric analysis water evolution data to estimate available water within the spore to produce hydrolysis reactions and the temperatures at which this water becomes mobile
- Review the probability of kill model based on the enzyme threshold killing mechanisms of *B.a* spores and extend to an enzyme fitness model using a beta distribution rather than Gaussian representation
- Numerically model the DNA repair mechanism within the spore and develop a probability of kill model based on the DNA critical threshold, DNA repair process, exposure time, temperature, viable repair enzymes, and outgrowth times.

1.5 Overview

The model development will be presented in the following manner. Chapter 2 will review Captain Knight's water mobility model. Chapter 3 describes the two types of water released within the spore due to heating. The thermogravimetric analysis conducted will be used in this chapter to determine the temperatures at which these waters are

available within the spore for hydrolysis reactions. Chapter 4 reviews the probability of kill model and extends that ideal to employ the more physically realistic beta distribution. Chapter 5 examines the model of the spore's probability of survival after the thermal inactivation treatment. Since the spore's DNA is damaged, the damage DNA must be repaired in order to synthesize the enzymes and produce outgrowth. Chapter 5 will also describe and present results from the probability of kill model based on the concentration of repair enzymes available for the DNA repair process. Chapter 6 will give the conclusions and future work.

2. Spore Structure and Dynamics

2.1 Introduction

The spore's strong resistance to heat and chemicals is primarily due to the properties of multiple layers that make up the spore. These layers protect the spore's DNA from damage by acting as a diffusion barrier and by dehydrating the spore's core where the DNA resides. During the thermal inactivation process, water within the spore becomes mobile and can react with molecules. In addition to pyrolysis reactions in which bonds that hold the molecule together break by heating, the mobile water can also cause hydrolysis damage to the spore's DNA and enzymes. Further, the release and movement of molecular water is important for these hydrolysis reactions.

2.2 Spore Structure

The *Bacillus* spore is constructed of several layers including the exosporium, spore coat, germ cell wall, outer and inner membrane, cortex, and core. The structure and chemical composition of the spore play major roles in spore resistance. Figure 2.1 shows an illustration of the major layers of a *Bacillus* spore (note that layers are not drawn to scale). The outermost layer is the exosporium. The exosporium is not present in spores of all *Bacillus* species. It contains mostly water, but also carbohydrates and proteins [33]. However, the exosporium is not believed to provide extra protection or heat resistance for the spore [16].

Beneath the exosporium is the spore coat made up largely of proteins. The spore coat protects the spore from destruction by lytic enzymes and many toxic chemicals. [33]. However, heat resistance is not provided by the spore coat [6].

Inside the spore coat lays the outer membrane. Although the outer membrane is important in spore formation, in the dormant spore the function of this membrane is not clear [33]. However, like the spore coat the outer membrane "has no notable effect of spore resistance to heat" [34].

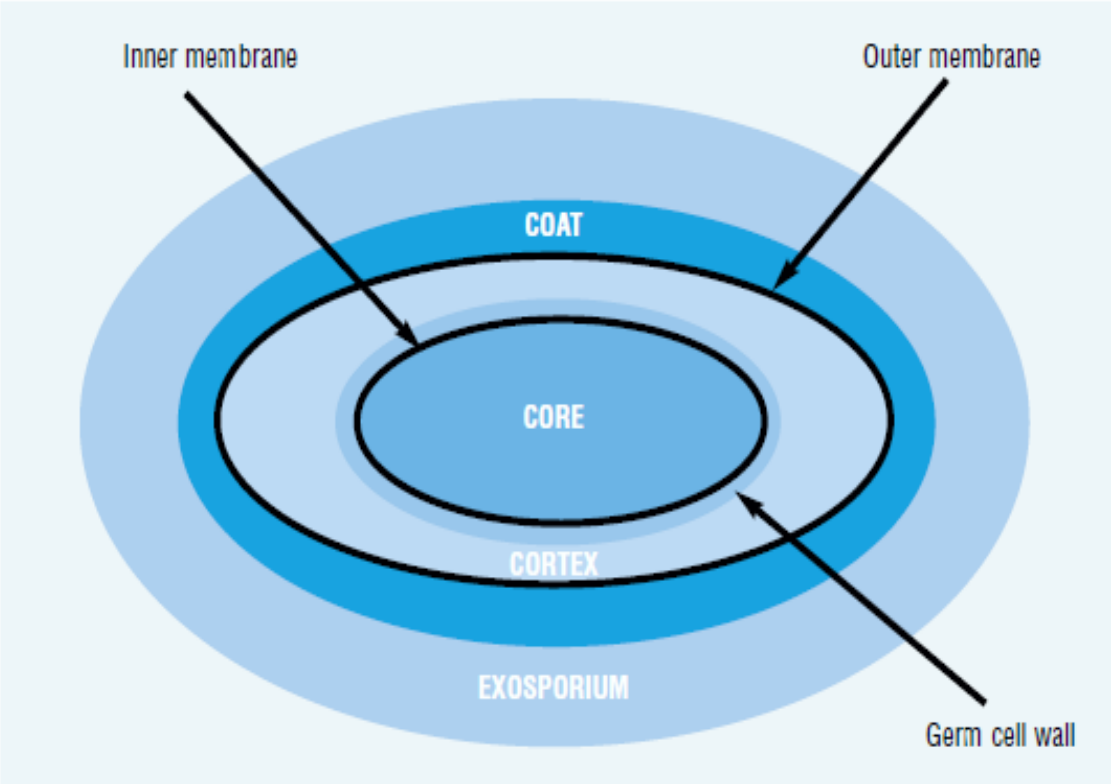

Figure 2.1: Spore Structure [33]

The next layer in the spore is the cortex which consists of peptidoglycan (PG). The cortex reduces the core water content which is essential to the spore's resistance to wet heating. The germ cell wall is also composed of PG. During germination, the germ

cell wall becomes the cell wall of the outgrowing cell. It does not provide any heat resistance for the spore [12, 34].

The inner membrane separates the core from the cortex and is relatively impermeable to small hydrophilic and hydrophobic molecules [33]. This membrane provides a strong permeability barrier to protect the core from damage.

In the center of the spore is the core. The core consists of the spore DNA and most spore enzymes. Depending on the species, the core's wet weight as water is only 25-55%. Additionally, the amount of free water is extremely low which indicates that molecular mobility within the core is almost nonexistent. The core water content plays a key role in spore resistance to wet heat and in the spore's enzymatic dormancy. The spore is more resistance to wet heat with low core water content [11]. The core water content is dependent on numerous things including sporulation condition, temperature, and spore preparation temperatures. For example, the higher the preparation temperature, the lower the core water content [23]. In high humidity conditions, more water accumulates in the regions external to the core. To understand the chemical reactions taking place within the spore, reaction kinetics concepts will be reviewed in the next section.

2.3 Reaction Kinetics

Reaction kinetics will be used throughout to describe damage reactions. Reaction kinetics, also known as chemical kinetics, is the study of rates of chemical processes. First-order reactions are ones that are directly proportional to the reactant concentration. The rate of the reaction is directly related to the concentration of the reactant by a

proportionality constant, k. The rate constant for thermal reactions satisfies an Arrhenius equation, that is

$$k(T) = Ae^{-\frac{E_a}{RT}} \tag{2.1}$$

where A is the encounter frequency, E_a is the activation energy, R is the gas constant, and T is absolute temperature. Therefore, the rate constants increase with increasing temperature. The reaction rates are influenced by the physical state of the reactants, the concentration of the reactants, the temperature at which the reaction occurs, and the presence of any catalysts in the reaction. For example, later in Chapter 4, the rate of enzyme damage has been modeled as

$$\frac{dE}{dt} = -k_1(T)E - k_2(T)[H_2O](t,T)E \tag{2.2}$$

where

E = spore's enzyme concentration

$[H_2O]$ = average water concentration

k_1 = rate coefficient associated with enzyme breakdown during pyrolysis thermal damage

k_2 = rate coefficient associated with enzyme breakdown during hydrolysis damage.

The units of enzyme and average water concentrations are in molal units. Molal is the number of moles of solute per kilogram of solvent. Activation energies for hydrolysis reactions are generally smaller than those for pyrolysis reactions. Therefore, it can be seen that, since water plays an important role in the chemical kinetics of thermal damage, the water mobility can be a significant influence on thermal damage within the spore.

2.4 Water Mobility Model

Using the knowledge of the role of each layer in the spore with respect to heat resistance, Captain Knight developed a model to illustrate the mobility of water within the spore. This water mobility model was based on a diffusion equation (Equation 2.3) where only the spore's core and cortex was considered in a two-layer spore model [19], and is given by

$$\frac{\partial w}{\partial t} = f(w) + \nabla \bullet D \nabla w \tag{2.3}$$

where

w = concentration of mobile water (molal)

t = time (sec)

f (w) = production of water (molal/sec)

D = diffusion coefficient (cm^2/sec).

In the water mobility model, since the core initially contains an extremely low amount of absorbed water, it was assumed that the concentration of absorbed water in the core is zero. Thus, the water content in the core was assumed to be only chemically bound water. Whereas, the cortex contains absorbed and chemically bound water molecules. It was assumed an equal amount of chemically bound water is available throughout the core and cortex.

The absorbed and chemically bound water molecules become mobile in a free molecular state, similar to a gaseous state, when the spores are heated.

$$[H_2O]_l + Heat \rightarrow [H_2O]_g$$
$$[H_2O]_b + Heat \rightarrow [H_2O]_g$$

where

$[H_2O]_l$ = initial concentration of absorbed water molecules (molal)

$[H_2O]_b$ = initial concentration of chemically bound water molecules (molal)

$[H_2O]_g$ = initial concentration of mobile water molecules (molal).

The two types of mobile water are energized at different temperatures. These temperatures will be estimated in the Chapter 3 thermogravimetric analysis.

For the water mobility model, the initial distribution of mobile water in the spore is the following,

$$w(r,0) = [H_2O]_g(r) \tag{2.4}$$

where r is the radius.

Since water is consumed through reaction with hydrocarbon compounds within the spore, the production term in Equation 2.3 was reduced to a simple first order reaction term:

$$f(w) = -k_t w \tag{2.5}$$

where k_t is the average rate for all possible hydrolysis reactions in the spore. The rate coefficient again satisfies the Arrhenius equation given in Equation 2.1.

In the water mobility model, it was assumed that the spore is spherically symmetric. Therefore, the model becomes one dimensional with respect to the radius of the spore and time ($w(r, t)$). The diffusion of water was modeled radially from the spore's coat into the cortex and the surrounding environment. At the boundary where the radius is equal to zero, the solution must be finite, that is,

$$|w(0,t)| < \infty.$$

When the radius is equal to the total spore radius ($r = r_0$), the flow of water across the outside boundary is proportional to the water content in the spore at the outer boundary and ambient humidity. This boundary condition was modeled by,

$$-\hat{n}.D\nabla w(r_0,t) = h\{w(r_0,t) - [H_2O]_a\} \tag{2.6}$$

where

$\hat{n}$ = outward normal vector

$[H_2O]_a$ = water concentration outside spore (molal)

h = surface flow velocity.

For spherical geometry, $\hat{n}$ became the outward radial direction. Therefore, Equation 2.4 became

$$-D\frac{\partial w}{\partial r}(r_0,t) = h\{w(r_0,t) - [H_2O]_a\}. \tag{2.7}$$

Since the diffusivity, *D*, was assumed to remain constant across the radius of the spore, the diffusion term in Equation 2.3 became

$$\nabla.D\nabla w = D\left(\frac{\partial^2 w}{\partial r^2} + \frac{2}{r}\frac{\partial w}{\partial r}\right). \tag{2.8}$$

In order to find the analytical solution to the water mobility model, dimensionless variables were chosen. Refer to Ref. 19 for additional details pertaining to these variables. Introducing these variables gives the following expression,

$$\frac{\partial \nu}{\partial \tau} = -\beta\nu + \frac{1}{x^2}\frac{\partial}{\partial x}(x^2\frac{\partial \nu}{\partial x}) \qquad 0 < x < 1, \tau > 0 \tag{2.9}$$

with boundary conditions

$$\frac{\partial \nu}{\partial x}(0,\tau) = 0 \qquad\qquad \tau > 0 \tag{2.10}$$

$$-\frac{\partial v}{\partial x}(1,\tau) = B(v(1,\tau) - \gamma) \qquad \tau > 0 \qquad (2.11)$$

The initial condition

$$v(x,0) = \alpha_1(x) f_1(T^*) + \alpha_2(x) f_2(T^*) \qquad 0 < x < 1 \qquad (2.12)$$

The dimensionless constants are

$$B = \frac{r_o h}{D}, \qquad \beta = \frac{r_0^2 k_t}{D}, \qquad \text{and} \qquad \gamma = \frac{[H_2O]_a}{[H_2O]_M}$$

with functions

$$\alpha_1(x) = \frac{[H_2O]_l(r_0 x)}{[H_2O]_M} \qquad \text{and} \qquad \alpha_2(x) = \frac{[H_2O]_b(r_0 x)}{[H_2O]_M}.$$

Using separation of variables, the homogenous problem given in Equation (2.7) and the homogenous boundary conditions became

$$h'(\tau) + (\beta + \mu)h(\tau) = 0 \qquad (2.13)$$

$$[x^2 g'(x)]' + \mu x^2 g(x) = 0 \qquad (2.14)$$

$$g'(0) = 0 \qquad (2.15)$$

$$-g'(1) = Bg(1) \qquad (2.16)$$

where μ is a separation parameter. The eigenvalues and eigenfunctions were found by solving Equations 2.14, 2.15, and 2.16 with respect to the homogenous boundary conditions. Further details are outlined in Ref.19 page 3-14 and 3-15.

The solution to the homogenous system is the following,

$$v(x,\tau) = \sum_{n=1}^{\infty} F_n(T^*) e^{-w_n \tau} g_n(x) + \gamma \sum_{n=1}^{\infty} \langle 1, g_n \rangle \frac{s_n^2}{w_n} [1 - e^{-w_n t}] g_n(x). \qquad (2.17)$$

The first series represents the influence of the initial water distribution while the second series represents the influence of the wet or dry heating environment. Since the DNA is

only present in the spore core, all hydrolysis reactions with DNA will occur in the core. The average total mobile water concentration in the core was given by

$$[H_2 0]_c(t) = \frac{3}{r_c^3} \int_0^{r_c} w(r,t) r^2 dr . \tag{2.18}$$

Substituting Equation 2.17 and dimensionless variables into Equation 2.18 yields

$$[H_2O]_c(t_c\tau) = \frac{3}{x_c^3}[H_2O]_M \left\{ \sum_{n=1}^{\infty} F_n(T^*) G_n(x_c) e^{-w_n \tau} + \gamma \sum_{n=1}^{\infty} G_n(1) G_n(x_c) \frac{s_n^2}{w_n} [1 - e^{-w_n t}] \right\}. \tag{2.19}$$

Physically, Equation 2.19 states that for short exposure times, the second term approaches zero. This implies that the first term dictates the release, diffusion, and reaction of water in the core. During long exposure times, the effect of the water concentration outside the spore becomes relevant [19]. For additional details about the water mobility model see Ref. 19 Appendix B.

Captain Knight's water mobility model will be used to characterize the spore's chances of survival during the inactivation process. The spore's survival is dependent on hydrolysis and pyrolysis reactions occurring within the spore during the thermal heating. Chapter 3 Thermogravimetric Analysis will focus on the concentration of water within the spore and the temperatures at which this water will be available for hydrolysis reactions.

3. Thermogravimetric Analysis

3.1 Introduction

Two types of water are contained within the spore, absorbed and chemically bound water. Absorbed water, weakly associated with cell materials, is located in the spore's cortex while chemically bound water is located in the spore's core and cortex. During the inactivation of the spore, the absorbed and chemically bound water molecules become mobile. The weakly bound absorbed water becomes energized and mobile at lower temperature than strongly held chemically bound water. Captain Knight assumed these temperatures were around 100 ^{o}C for absorbed water and 300 ^{o}C for chemically bound water [19]. In order to confirm these assumptions and approximate the percentage of water in the *Bacillus* spore, thermogravimetric analysis studies were conducted by Dr. Felker [10]. Dr. Felker used *Bacillus thuringiensis* when conducting this analysis. The percentage of water in the spores is important during the inactivation process; the diffusion of water allows hydrolysis reactions to occur within the spore. These reactions are important in the inactivation of the spore because they lead to deploymerization reactions of the spore's DNA and enzymes. Damage to the DNA and to enzymes influence the DNA repair process and the spore's ability to produce outgrowth as well as the repair time to produce outgrowth.

3.2 General Discussion

Thermogravimetric analysis (TGA) is a thermal analysis technique that measures the weight change in a material as a function of temperature and time under a controlled

atmosphere [38]. Thus, TGA can directly measure the weight loss of a material with temperature or time, as such loss is due to dehydration or decomposition as the temperatures ranges from ambient to 1000^{o}C. TGA can be used in multiple applications, such as, thermal stability or degradation investigation of organic/inorganic materials and inert/oxidative atmospheres, determining of organic/inorganic content of mixtures, phase transition measurement, reaction kinetics with reactive gases, and pyrolysis kinetics [38].

The TGA of solids relies on a high degree of precision in three measurements: weight, temperature, and temperature change. The analysis is carried out by raising the temperature gradually and plotting percentage of weight change against temperature [28, 38]. The thermogravimetric analyzer consists of a high precision balance with a platinum pan loaded with a sample. The platinum pan is rigidly attached to the end of the balance arm in the horizontal configuration, and there is no added mass due to a suspension harness. According to Menczel et al, "suspension below the balance may be less rigid and does not recognize the compensating weight and thus detracts less from the available range" [24]. The sample is placed in a small electrically heated oven with a thermocouple to accurately measure the temperature. A computer is used to control the instrument.

TGA can provide a quantitative measurement of the weight change but cannot indicate the nature of the material lost. Therefore, evolved gas analysis (EGA) measurements can be done. EGA gives the nature of the changes in the gas phase. It can be qualitative or quantitative measurements. Mass spectroscopy (MS) or Fourier transform infrared spectroscopy (FTIR) can be applied to the EGA [24]. For our analysis Dr. Felker used FTIR. The FTIR system allowed Dr. Felker to confirm that the major volatile associated with the mass change was indeed water.

3.3 Thermogravimetric Analysis Data

3.3.1 Raw TGA Data.

There are two types of TGA, differential and normal. The normal TGA method was used for our study. The sample can be in various atmospheres including oxidizing and non-oxidizing. An oxidizing atmosphere is one in which oxygen is present whereas in a non-oxidizing atmosphere oxygen is not present. For this study, *Bacillus thuringiensis* (B.t) was focused on. The *B.t* sample was in a quasi-wet state and slowly dried. Therefore, the study has a steady state measurement of all excess water. Although, there is water located on the outside of the sample and within the spores, this study is only concerned with the water within the spores. As the sample is heated, several things can happen. The sample can stay the same, lose mass, or gain mass. Also, as the sample is heated, more than one process is occurring. There is an early release of water and at later temperatures combustion is released from the sample.

The TGA raw data obtained from using *B.t* can be seen in Figure 3.1. The blue curve represents the weight change in the sample as a function of time (seconds). The green curve shows the increase in temperature with time. The temperature increases linearly at a rate of 0.2 ^{o}C per second. Also, there are distinct slope variations in the mass as time increases.

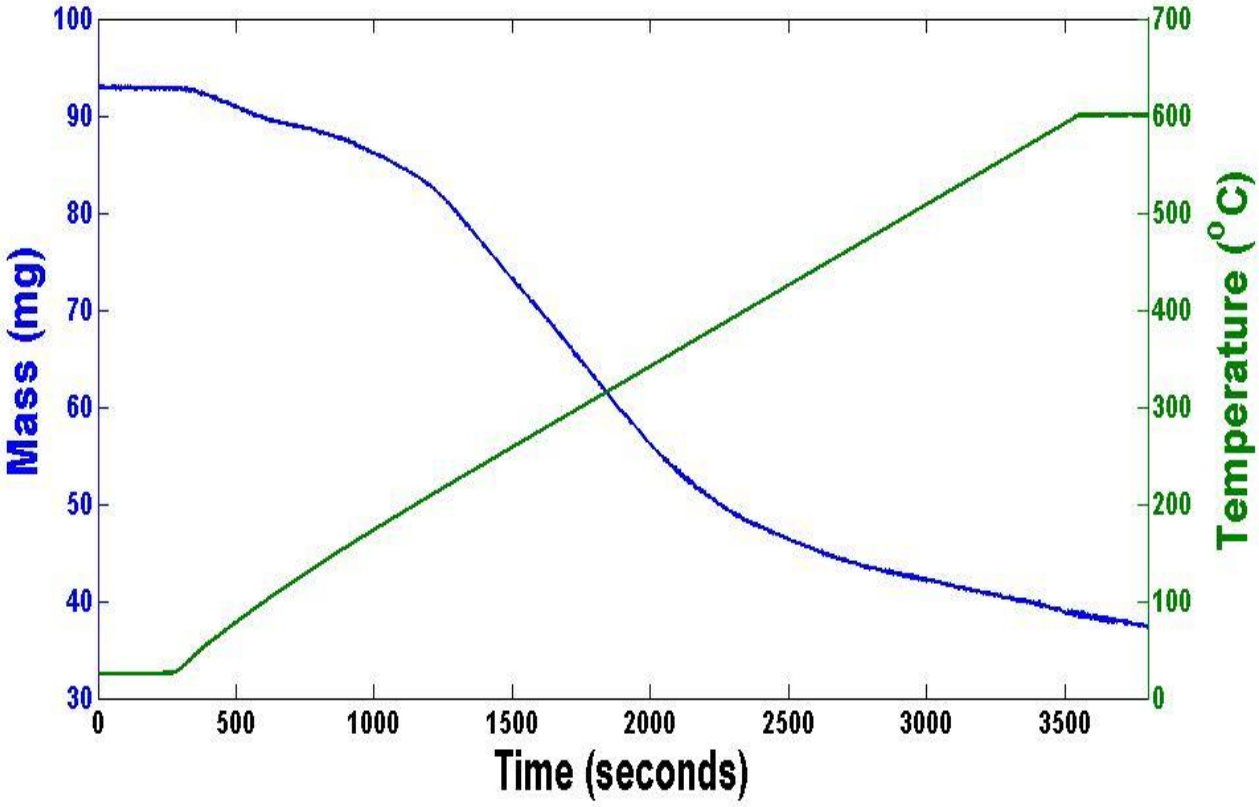

Figure 3.1: TGA Raw Data

For use in this study, the TGA data was represented by mass change as a function of temperature. This is the blue curve depicted in Figure 3.2. This curve depicts steep slopes between 55°C and 125°C and between 200°C and 350°C. These steep slopes indicate a rapid loss of mass in these temperature ranges. This mass loss is related to the release of water from the sample.

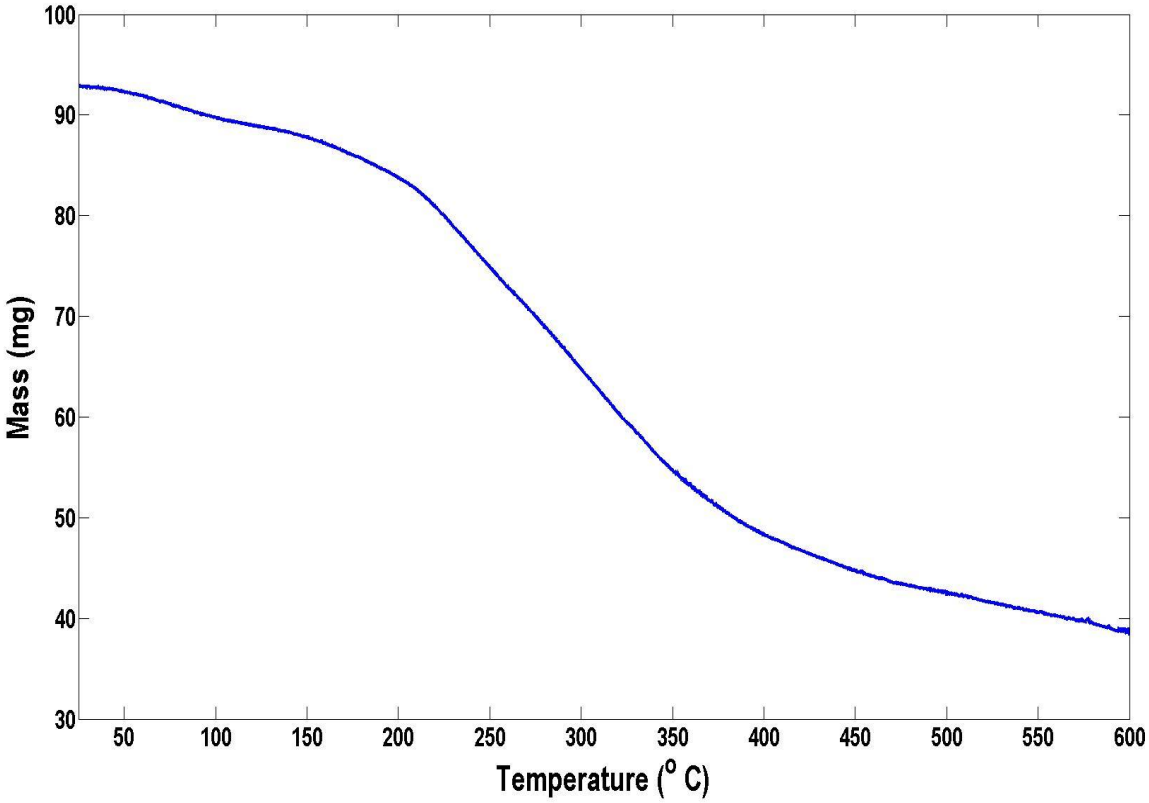

Figure 3.2: TGA Raw Data Mass Loss versus Temperature.

3.3.2 Modeling Data.

In order to estimate the amount of absorbed and chemically bound water released from spores at selected temperatures, a model was built to provide the best fit to the TGA experimental data (blue curve in Figure 3.2). Gaussian density functions were chosen to represent the distributions of absorbed water, chemically bound water, and other chemical processes. Each Gaussian density function is centered about their respective mean release temperature, T_1, T_2, and T_3 with associated standard deviations σ_1, σ_2, and σ_3.

$$f_i(T) = \frac{1}{\sigma_i \sqrt{2\pi}} e^{-\frac{1}{2}\left(\frac{T - T_i}{\sigma_i}\right)^2} \qquad i = 1,2,3.$$

The total mass, $G(T^*)$, released at any given temperature, T^*, is determined by integrating the weighted sum of the Gaussian density functions, that is,

$$G(T^*) = \int_{-\infty}^{T^*} w_1 f_1(\tau) + w_2 f_2(\tau) + w_3 f_3(\tau)\, d\tau$$

$$= w_1 F_1(T^*) + w_2 F_2(T^*) + w_3 F_3(T^*) \tag{3.1}$$

where

$$F_i(T^*) = \frac{1}{2}\left[1 + erf\left(\frac{T^* - T_i}{\sigma_i \sqrt{2}}\right)\right], \qquad i = 1,2,3. \tag{3.2}$$

Here w_1 represents the total amount of absorbed water available for release, w_2 represents the total amount of chemically bound water available for release, w_3 represents the total amount of other chemical processes available for release, and *erf* is the error function.

The TGA model is then expressed by subtracting the total mass released at any temperature, $G(T^*)$, from the total mass of the sample, TM, i.e.

$$TGA_f(T^*) = TM - G(T^*) \tag{3.3}$$

where

$$TM = w_1 + w_2 + w_3.$$

Furthermore, how much water is released at any temperature from the spore, $[H_2O]_s(T^*)$, can be determined by subtracting the total available water, $[H_2O]_A$, released at any temperature from the total mass of the sample,

$$[H_2O]_s(T^*) = TM - [H_2O]_A(T^*) \tag{3.4}$$

where

$$[H_2O]_A = w_1F_1(T^*) + w_2F_2(T^*).$$

3.3.3 Results.

Using the TGA model, the appropriate values that give the best fit approximation to the TGA experimental data curve. These values are outlined below in Table 3.1.

Table 3.1: Parameters for TGA Curve Fit

	Weighted Coefficient (w_i)	**Mean Temperature (T_i)**	**Standard Deviation (σ_i)**
Absorbed Water	5	105	60
Chemically Bound Water	38	290	70
Other Chemical Processes	50	815	300

The three weighted Gaussian density functions are illustrated in the Figure 3.3 using the values from Table 3.1. The majority of absorbed water is mostly likely released in a neighborhood of 105 ^oC until all the absorbed water is active. Then the chemically bound water most likely begins its release to a peak of 290 ^oC. The other chemical processes which reduce the mass are mainly released to a peak of 815 ^oC.

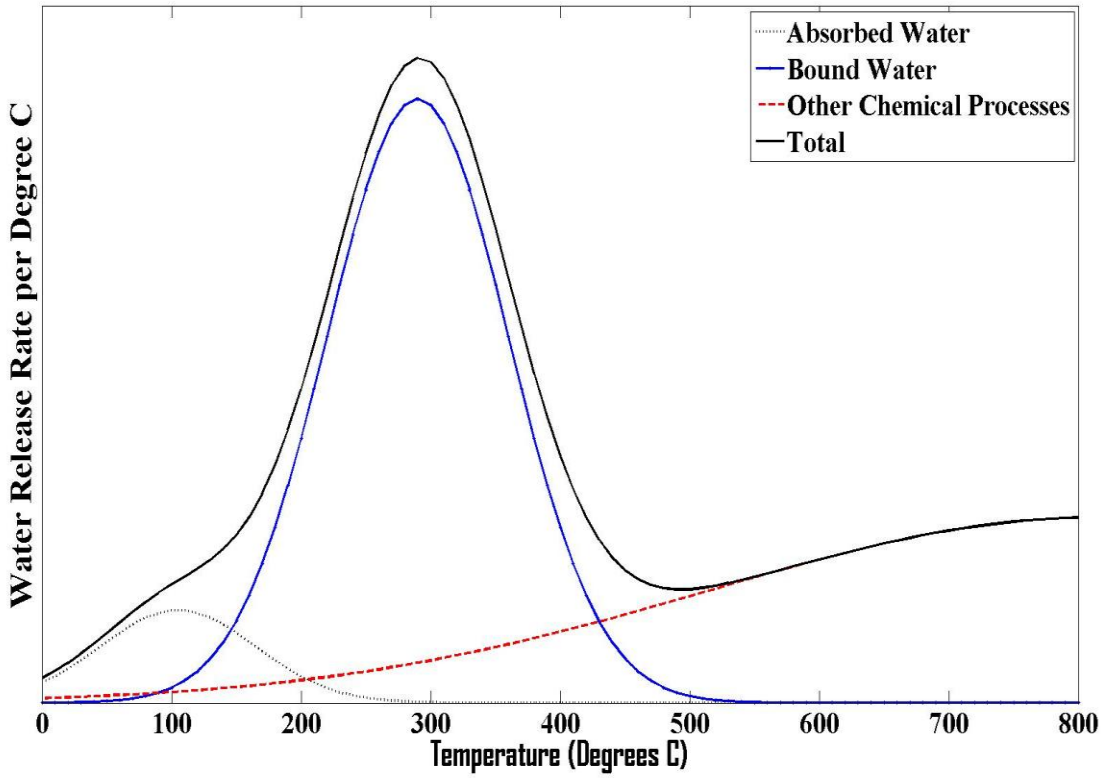

Figure 3.3: Weighted Gaussian Density Functions

Figure 3.4 shows the results of our best fit approximation to the TGA data using the values in Table 3.1. This figure depicts the release of mass from the sample as temperature increases. The blue curve represents the true TGA experimental data, the solid red line represents our best fit model to the TGA data, and the dashed red line represents the amount of mass loss due to water only.

From probability theory, the empirical rule states that for a Gaussian distribution [12],

68% of the measurements lie within $\mu \pm \sigma$

95% of the measurements lie within $\mu \pm 2\sigma$

97.7% of the measurements lie within $\mu \pm 3\sigma$

where μ represents the mean and σ represents the standard deviation. Therefore, since our best fit model gives a close approximation to the TGA experimental data, 68% of absorbed water is released approximately between 45°C and 165°C while 68% of the chemically bound water is released approximately between 220°C and 360°C. Also, our results support Captain Knight, assumptions that the absorbed water becomes available around 100°C and chemically bound water becomes available around 300°C.

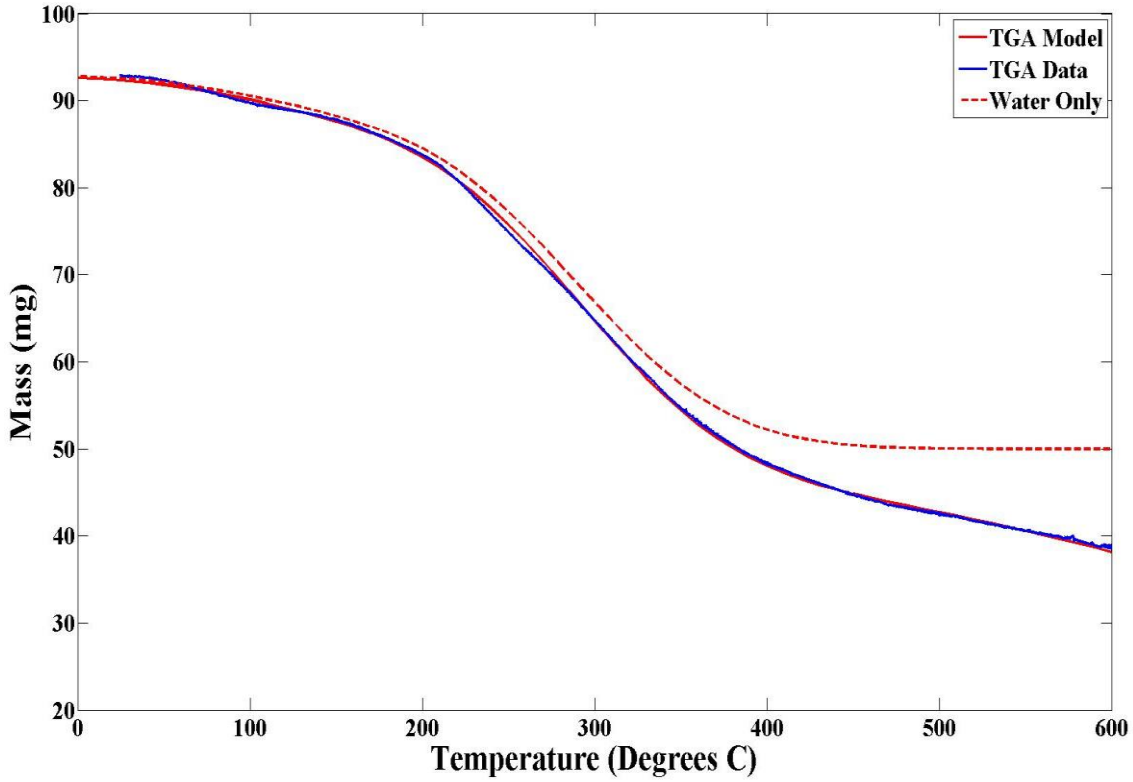

Figure 3.4: TGA Model Fit

Figure 3.5 shows the percent mass loss as temperature increases. Approximately 2% of the sample's weight is loss around 105°C and 25% is loss around 290°C. Furthermore, by 430°C all of the sample's water is released and that approximately 40-45% of the sample's weight is water. The percentage of water within the spore is

important for hydrolysis reactions to occur. The higher percentage of water implies increase hydrolysis reactions can occur. During the heating process of the *Bacillus* spores, hydrolysis reactions are an important aspect to inactivating the spores.

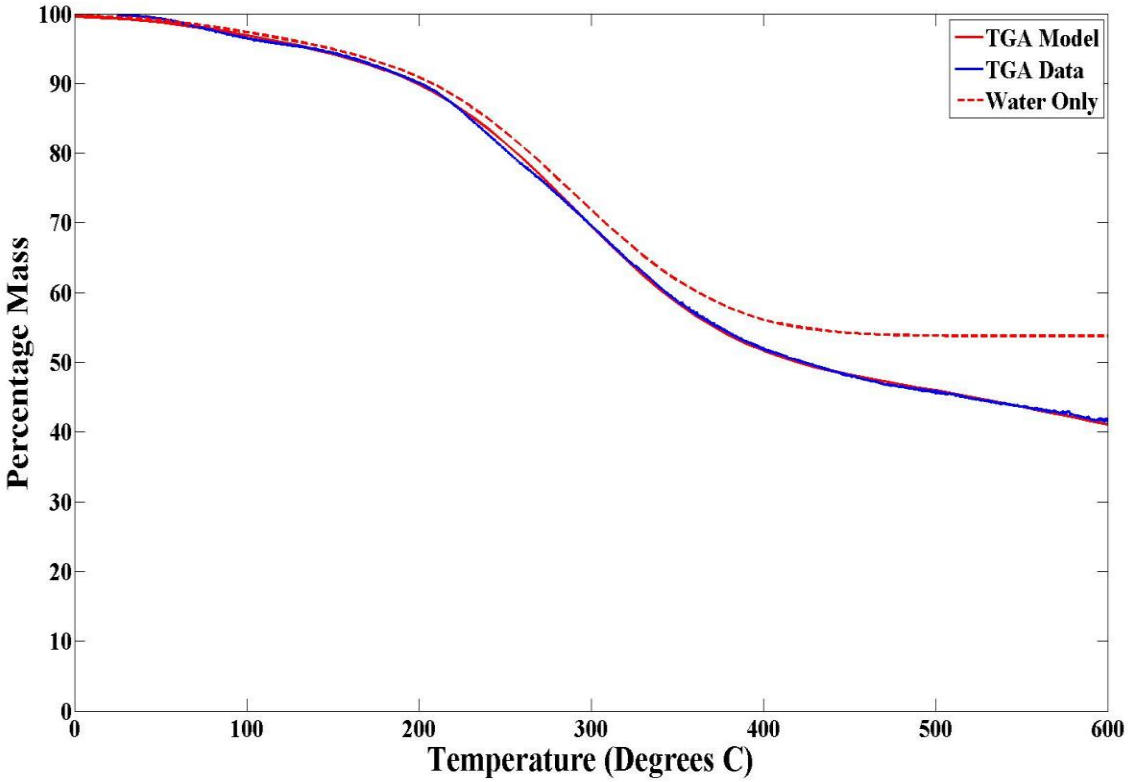

Figure 3.5: TGA Model Fit (Percent Mass Loss)

4. Spore Damage and Repair Mechanisms

4.1 Introduction

In Chapter 3, the study observed that approximately 40-45% of the spore's weight is water. Water plays an important role in the inactivation of the spores. The transport of water throughout the spore allows hydrolysis reactions to occur in the core. The hydrolysis reactions can cause damage to the spore DNA and enzymes which leads to the spore death if the DNA is not repaired. In the spore population, it is assume that each spore contains a full complement of DNA and a concentration of enzymes adequate for germination. It has been assumed that the damage repair capability for a spore in the spore population is a sample from a certain initial enzyme fitness distribution. When the enzyme damage accumulates, this fitness distribution is degraded. Once degradation is beyond some critical level, the spore cannot repair the damaged DNA and therefore, cannot germinate or produce outgrowth. Probability of kill models based on water mobility, hydrolysis, DNA information content, and the spore's enzyme fitness levels have been created to further explore the spore's chance of survival.

4.2 Spore Damage Model

4.2.1 Hydrolysis & Pyrolysis.

Hydrolysis is the reaction of a molecule with water. At low temperatures, hydrolysis reactions can occur because of their low activation energy. Hydrolysis can be catalyzed by hydrogen ions in low pH or by hydroxide ions in high pH, where the pH of an aqueous solution is the logarithm of the reciprocal of the concentration of hydrogen

ions in the solution. A solution with a pH below seven is acidic and a pH above seven is basic; neutral solution has pH equal to seven. So hydrolysis rates increase in strongly basic or strongly acidic solution.

(Note that: $k_{(\text{hydrolysis})} = k_{(\text{acid catalysis})}[H^+] + k_{(\text{neutral})}[H_2O] + k_{(\text{base catalysis})}[OH^-]$) [32]

Bacteria can survive in an environment with pH measurements between five and eight, so acid hydrolysis is somewhat less damaging than basic hydrolysis paralleling the pH dependence of hydrolysis rates for most organic molecules that are susceptible to hydrolysis for which $k_{(\text{acid catalysis})} < k_{(\text{base catalysis})}$.

Autoionization is a reaction in which water molecules dissociate into hydrogen cations (H^+) and hydroxide anions (OH^-) in an equilibrium process. That is,

$$H_2O \rightleftharpoons H^+ + OH^-.$$

The equilibrium constant (K) for this dissociation of water is defined as

$$K = \frac{[H^+][OH^-]}{[H_2O]}.$$

The pH in a solution is related to its acidity or basicity. pH is defined as

$$\text{pH} = -\log[H^+]$$

where $[H^+]$ is in molarity (M). The concentration of hydroxide ions in the solution, given by

$$\text{pOH} = -\log[OH^-]$$

can be derived from pH using the equilibrium constant (K). Define a new constant, K_W, such that

$$K_W = K[H_2O] = [H^+][OH^-].$$

Then

$$K_W = [H^+][OH^-],$$
$$\Rightarrow [OH^-] = \frac{K_W}{[H^+]}.$$

Therefore,

$$-\log[OH^-] = -\log\frac{K_W}{[H^+]},$$
$$= -\log K_W + log[H^+],$$

$$\Rightarrow \text{pOH} = -\log K_W - \text{pH}.$$

The change in pH within the spore can cause damage to the spore DNA by hydrolysis. For example, as pH approaches 9, the DNA double helix begins to dissociate into its component single strands. This is because the hydroxide ions can react with bases in DNA base pairs to remove certain protons enhancing the rate of reaction of the bases with water. Acids can accelerate the rate of reaction of DNA bases with water by donating a proton to the bases. Therefore, certain chemicals that alter spore pH may be effective to cause DNA damage which can lead to spore death.

Pyrolysis is the thermal decomposition of organic materials within the spores. These damage reactions are mediated by radical formation, abstraction and recombination reactions. Pyrolysis usually occurs at much higher temperatures than do hydrolysis reactions except in the extreme absence of water.

4.2.2 Types of Damages to DNA and enzymes.

DNA and enzymes are biopolymers having very different structures and very different functions. DNA is the information storage medium that encodes the recipe for making all cellular polymers, including the enzymes. Enzymes are active proteins which

catalyze specific chemical reactions necessary to build biopolymers and disassemble them to generate energy.

DNA is a linear polymer made up of four different types of monomers. It has a fixed backbone which is built of repeating sugar-phosphate units. Each sugar is connected to one of four possible bases: adenine (A), cytosine (C), guanine (G), and thymine (T). In 1953, James Watson and Francis Crick correctly proposed that the DNA molecule consist of two stands bound together in a double helix through specific hydrogen bonding affinities of complementary bases for each other. The double helix structure is arranged such that the sugar-phosphate backbone lies on the outside and the bases on the inside. The bases form specific base pairing held together by hydrogen bonds: adenine (A) pairs with thymine (T) and guanine (G) pairs with cytosine (C). The sequence of bases along the DNA strands is the manner that genetic information is stored. The DNA sequence also determines the sequences of the ribonucleic acid (RNA) and protein molecules. If the DNA double helix is separated into two single strands, each strand can act as a template for replication. For perfect encoding of information, the loss of a single base in one DNA strand can be recognized by reading the complementary base and so the total information in the double helix is not degraded if the loss is recognized and repaired.

During the thermal inactivation of the spores, there are numerous types of reactive processes that can lead to DNA damage. Some include chemical modification such as alkylation or oxidation and base removal [35]. However, not all regions of DNA within the spore are important for spore survival and replication. Therefore, only damage to the critical or essential DNA necessary for germination and outgrowth is considered.

Proteins are linear polymers. Proteins are built from 20 amino acids and fold up into elaborate three-dimensional structures determined by their amino acid sequences. Enzymes are proteins folded into three-dimensional structures that can catalyze specific chemical reactions. DNA genes encode the sequences of proteins. The gene is the fundamental unit of hereditary information encoding a series of 3-bit letters or codons. A codon, a set of three bases along the DNA strand, determines the identity of one amino acid within the protein sequence. One incorrect amino acid can dramatically alter the function of the protein. The three bits of ordered information allow 64 possible encoding combinations. The capability of the three-bit letter is sufficient to encode for the 20 amino acids. Therefore, there is redundancy in the code. As a result, removing or altering the third base pair in the sequence in a codon may or may not destroy the information content. Whereas, removing the first base in a codon most likely will cause problems [19]. Some codon letters are inactive, so destroying that information will cause no degradation in the useful DNA gene information or proteins function encoded by that gene.

As previously stated, spore DNA and enzyme damage can occur in many ways. According to Setlow "chemicals such as nitrous acid or formaldehyde can kill the spores by DNA damage, while others, such as oxidizing agents, appear to damage the spore's inner membrane so that this membrane ruptures upon spore germination and outgrowth" [34]. Water can react with DNA and proteins resulting in deploymerization. Deploymerization is breaking a large strand of polymers into two smaller ones. Water more frequently reacts with DNA causing deamination and depurination damage. Deamination is the removal of amino group from the DNA's base pair. This type of

damage can prevent the DNA from replicating properly. The major type of deamination reaction converts cytosine (C) to an altered DNA base, uracil (U), but deamination occurs on other bases as well.

Denaturation is the reaction in which the proteins lose their structure. The proteins lose their structure by application of some external stress, such as heat or a strong acid or base. Following denaturation, however, some proteins will return to their native structure under proper conditions. Although, under extreme conditions usually cause irreversible change and the protein can no longer perform its function once it has been denatured.

Depurination is an alteration of DNA in which the purine base (adenine or guanine) is removed from the DNA chain. Depurination damage is most common since the purine bond is especially susceptible to hydrolysis.

When DNA is missing one of its base pairs, the DNA strand cannot match up with its other half of the helix chain. Removal of a DNA base can have a range of effects depending on the information content of the codon. For this research, only damage which reduces the information content in critical or essential codon, which contain information necessary to replicate the spore during germination. Also, it has been assumed that hydrolysis reactions are equally likely to occur at all protein sites and that the critical threshold damage to DNA caused by depurination is equally likely for all base pair sites [19].

4.2.3 DNA Repair Mechanisms.

DNA repair is a complex system of interacting biomolecular processes. The DNA repair pathways have evolved but are partially conserved in all life, from bacteria to mammals [36]. Each repair pathway is directed to a specific type of damage, and several

pathways can target a given type of damage. Major DNA repair pathways include base excision repair (BER), nucleotide excision repair (NER), mismatch repair (MMR), homologous recombinational repair (HR), and non-homologous end joining (NHEJ). Each repair pathway requires a number of repair enzymes for the process.

BER is the main mechanism for removing spontaneous DNA lesions that are caused by hydrolysis or oxidation. This repair process removes damaged bases from DNA through a multistep process in which the repair enzymes work independent of each other [37]. An example of BER is the repair of uracil-containing DNA. Recall that uracil can be formed in DNA by the deamination of cytosine.

NER removes bulky adducts in DNA or chemical bonds between bases of DNA. The mechanisms of NER are more complex than that of BER, but the basic principles are similar [37]. MMR provides protection against occasional rare errors that occur during DNA replication [8]. HR and NHEJ double-stand breaks. HR uses a homologous DNA template, is highly accurate, whereas NHEJ rejoins the broken ends without a template and is often accompanied by loss of some nucleotides [8].

As mentioned above, deamination and depurination is the reaction of water with the base pairs of DNA. Therefore, most likely during the thermal inactivation of the spores, the base pairs are damaged. Since BER is the main repair system for this type of damage, it will be assumed during germination that BER will be used to repair most of the damaged DNA, dominating the overall rate of repair. Further discussion will be given in Chapter 5.

4.2.4 Damage Model.

This research assumes that the spore starts out with 100% healthy DNA and this is degraded by exposure to heat due to hydrolysis and pyrolysis reactions. The rate of critical DNA damage can be modeled by the following rate equation,

$$-\frac{dI_D}{dt_e} = \tilde{k}_1(T)I_D + \tilde{k}_2(T)[H_20]_c(t_e,T)I_D \tag{4.1}$$

where I_D represents the critical DNA, $\tilde{k}_1$ is the rate coefficient associated with critical DNA breakdown during pyrolysis, $\tilde{k}_2$ is the rate coefficient associated with critical DNA breakdown during hydrolysis, t_e is the exposure time, T is temperature, and $[H_2O]_c$ is the average core water concentration given in Equation 2.19. The rate coefficients again satisfy the Arrhenius equation in Equation 2.1.

A simple solution to the rate equation is the following where the critical DNA diminishes exponentially,

$$I_D(t_e) = I_c f_D(T,t_e) \tag{4.2}$$

where $f_D(T,t_e) = e^{-\tilde{k}_1(T)t_e + \tilde{k}_2 H(t_e,T)}$ is the fraction of DNA remaining after some exposure time and temperature, $H(t_e) = \int_0^{t_e} [H_2O]_c(\tau)d\tau$, and I_c represents the initial state of critical DNA.

As the spore is heated, there is also damage occurring to the spore's enzymes. Since the enzymes are crucial for DNA repair, a damaged spore will only be able to germinate using the enzymes that survive the heating process. The damage to the DNA must be repaired before a viable cell is produced during outgrowth and there has to be a suitable amount of repair enzymes viable to accomplish this.

Let $E_r(t_e)$ be the enzyme concentration for the spore population at exposure, t_e. The rate of enzyme damage can be modeled by

$$-\frac{dE_r}{dt_e} = k_1(T)E_r + k_2(T)[H_20]_c(t_e,T)E_r \tag{4.3}$$

where k_1 is the rate coefficient associated with enzyme breakdown during pyrolysis and k_2 is the rate coefficient associated with enzyme breakdown during hydrolysis. These rate coefficients may not be the same rate coefficients associated with DNA damage. After integration, Equation 4.3 becomes

$$\begin{aligned} E_r(t_e) &= E_0 e^{-(k_1(T)t_e + k_2(T)H(T,t_e))} \\ &= E_0\ f(T,t_e) \end{aligned} \tag{4.4}$$

where, for simplicity,

$$f_E(T,t_e) = e^{-(k_1(T)t_e + k_2(T)H(T,t_e))}. \tag{4.5}$$

Equation 4.5 represents the fraction of remaining enzymes after a given exposure time and temperature.

4.3 Fitness Distribution Models

The spores' fitness distribution has been modeled with a Gaussian distribution representation [19]. In this section, this approach will be reviewed and extended the fitness model to a beta distribution representation.

4.3.1 Gaussian Model.

The Gaussian (Normal) distribution is the most widely used continuous probability distribution [12]. The Gaussian probability density function has the following representation with mean, μ and variance, σ^2,

$$f(x)=\frac{1}{\sigma\sqrt{2\pi}}e^{-\frac{(x-\mu)^2}{2\sigma^2}}, \qquad -\infty<x<\infty, \quad -\infty<\mu<\infty, \quad \sigma>0. \tag{4.6}$$

The Gaussian cumulative density function can be found by integrating equation 4.5,

$$P(x<x_0)=\Phi(x)\equiv\frac{1}{\sigma\sqrt{2\pi}}\int_{-\infty}^{x_0}e^{-\frac{(x-\mu)^2}{2\sigma^2}}dx. \tag{4.7}$$

A very important contributor to spore fitness is the store of enzymes in the spore that can serve to reconstitute an active cell. Prior to any heat treatment, the initial enzyme content, E_0, will be dependent on the initial state of the spore population. This initial state of enzymes will depend on numerous things. For example, spore preparation or sporulation will have an important role on the initial state. According to Melly et al, spore preparation temperature affects the core water content which in turn influences the spore's heat resistance [23]. Therefore, E_0 was drawn from a Gaussian fitness distribution with mean, μ_{E_0} and variance, $\sigma_{E_0}^{\ 2}$,

$$f(E_0)=\frac{1}{\sigma_{E_0}\sqrt{2\pi}}e^{-\frac{(E_0-\mu_{E_0})^2}{2\sigma_{E_0}^{\ 2}}}, \qquad -\infty<E_0<\infty, \quad -\infty<\mu_{E_0}<\infty, \quad \sigma_{E_0}>0.$$

The illustration of a notional enzyme fitness density function prior to heat is shown in Figure 4.1.

In order to repair damaged DNA, a certain amount of viable enzymes are needed. However, during the inactivation of the spore, damage is also done to the enzymes. Therefore, there must be a point at which there will be insufficient concentration of enzymes to repair the damaged DNA. This location is the critical kill threshold, E_k. Above this threshold, the spore contains the necessary enzymes needed for repair.

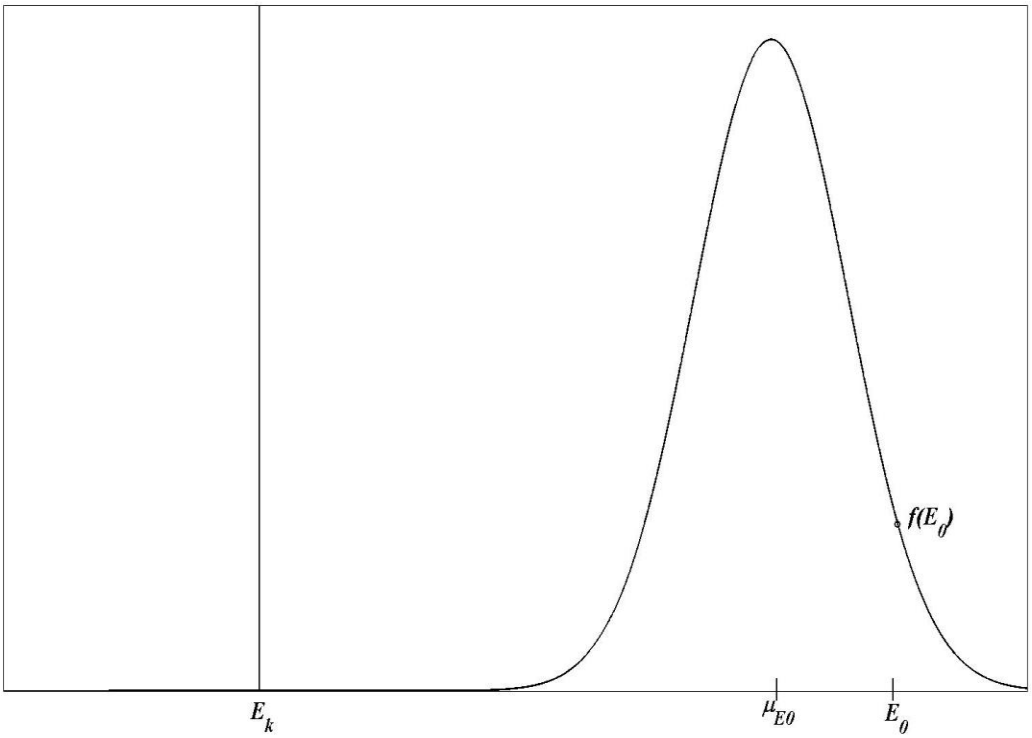

Figure 4.1: Enzyme Fitness Prior to Any Heating

As thermal exposure time progresses, the evolution of the distribution of $E_r(t_e)$ will approach the kill threshold. Since E_0 is a random variable, $E_r(t_e)$ is also a random variable drawn from a distribution with mean, μ_{E_r} and variance, $\sigma_{E_r}{}^2$.

From probability theory, the expectation of a continuous variable X is

$$E(X) = \int_{-\infty}^{\infty} x f(x) dx, \tag{4.8}$$

where f(x) is the probability density function for X. The mean and variance of a continuous distribution is defined in terms of expectations, that is

$$\mu = E[X]$$
$$\sigma^2 = E[(X-\mu)^2]$$

Expectation is a linear operator, that is

$$E[cX] = cE[X]$$
$$E[X_1 + X_2 + \cdots + X_n] = E[X_1] + E[X_2] + \cdots + E[X_n]$$

where c is a constant and $X_1, X_2, \ldots, X_n$ are continuous random variables [12].

Using these expectation properties, the mean of $E_r(t_e)$ is the following

$$\begin{aligned}\mu_{E_r} &= E[E_r(t_e)] \\ &= E[E_0 f_E(T, t_e)] \\ &= f_E(T, t_e) E[E_0] \\ &= f_E(T, t_e) \mu_{E_0}\end{aligned}$$

and variance of $E_r(t_e)$ is the following

$$\begin{aligned}\sigma_{E_r}^2 &= E[(E_r(t_e) - \mu_{E_r})^2] \\ &= E[(E_0 f_E(T, t_e) - f_E(T, t_e)\mu_{E_0})^2] \\ &= (f_E(T, t_e))^2 \; E[(E_0 - \mu_{E_0})^2]\end{aligned}$$

Using Equation 4.8,

$$\begin{aligned}E[(E_0 - \mu_{E_0})^2] &= \int_{-\infty}^{\infty} (E_0 - \mu_{E_0})^2 f(E_0) dE_0 \\ &= \int_{-\infty}^{\infty} (E_0 - \mu_{E_0})^2 \frac{1}{\sigma_{E_0}\sqrt{2\pi}} e^{-\frac{(E_0 - \mu_{E_0})^2}{2\sigma_{E_0}^2}} dE_0 \\ &= \frac{1}{\sigma_{E_0}\sqrt{2\pi}} \int_{-\infty}^{\infty} (E_0 - \mu_{E_0})^2 e^{-\frac{(E_0 - \mu_{E_0})^2}{2\sigma_{E_0}^2}} dE_0\end{aligned}$$

Using integration by parts method, $\int u dv = u.v - \int v du$, let

$$u = \frac{(E_o - \mu_{E_0})}{\sigma_{E_0}\sqrt{2\pi}} \qquad dv = (E_0 - \mu_{E_0}) e^{-\frac{(E_0 - \mu_{E_0})^2}{2(\sigma_{E_0})^2}} dE_0,$$

then

$$du = \frac{1}{\sigma_{E_0}\sqrt{2\pi}} dE_0 \qquad v = -\sigma_{E_0}{}^2 e^{-\frac{(E_0-\mu_{E_0})^2}{2(\sigma_{E_0})^2}}.$$

Thus,

$$E[(E_0-\mu_{E_0})^2] = -\frac{(E_o-\mu_{E_0})}{\sigma_{E_0}\sqrt{2\pi}}\sigma_{E_0}{}^2 e^{-\frac{(E_0-\mu_{E_0})^2}{2(\sigma_{E_0})^2}}\Big|_{-\infty}^{\infty} + \frac{1}{\sigma_{E_0}\sqrt{2\pi}}\int_{-\infty}^{\infty}\sigma_{E_0}{}^2 e^{-\frac{(E_0-\mu_{E_0})^2}{2(\sigma_{E_0})^2}} dE_0$$

$$= 0 + (\sigma_{E_0})^2 \int_{-\infty}^{\infty} \frac{1}{\sigma_{E_0}\sqrt{2\pi}} e^{-\frac{(E_0-\mu_{E_0})^2}{2(\sigma_{E_0})^2}} dE_0$$

$$= (\sigma_{E_0})^2.$$

Therefore,

$$\sigma_{E_r}^2 = (f_E(T,t_e))^2 \; E[(E_0-\mu_{E_0})^2]$$
$$= (f_E(T,t_e))^2 (\sigma_{E_0})^2.$$

Figure 4.2 depicts the evolution of the distribution of $E_r(t_e)$ as exposure time increases. The Gaussian function outlined in black represents the initial distribution of the enzyme content with mean, μ_{E_0} and variance, $\sigma_{E_0}{}^2$. The Gaussian function outlined in blue represents the distribution of the enzyme content after some exposure time, $t = \tau_1$ with mean, $\mu_{E_r}(\tau_1)$ and variance, $\sigma_{E_r}{}^2(\tau_1)$. The Gaussian function outlined in red represents the distribution of the enzyme content after additional heat exposure, $t = \tau_2 > \tau_1$ with mean, $\mu_{E_r}(\tau_2)$ and variance, $\sigma_{E_r}{}^2(\tau_2)$. As the exposure time increases, the mean of the distribution decreases as does the variance.

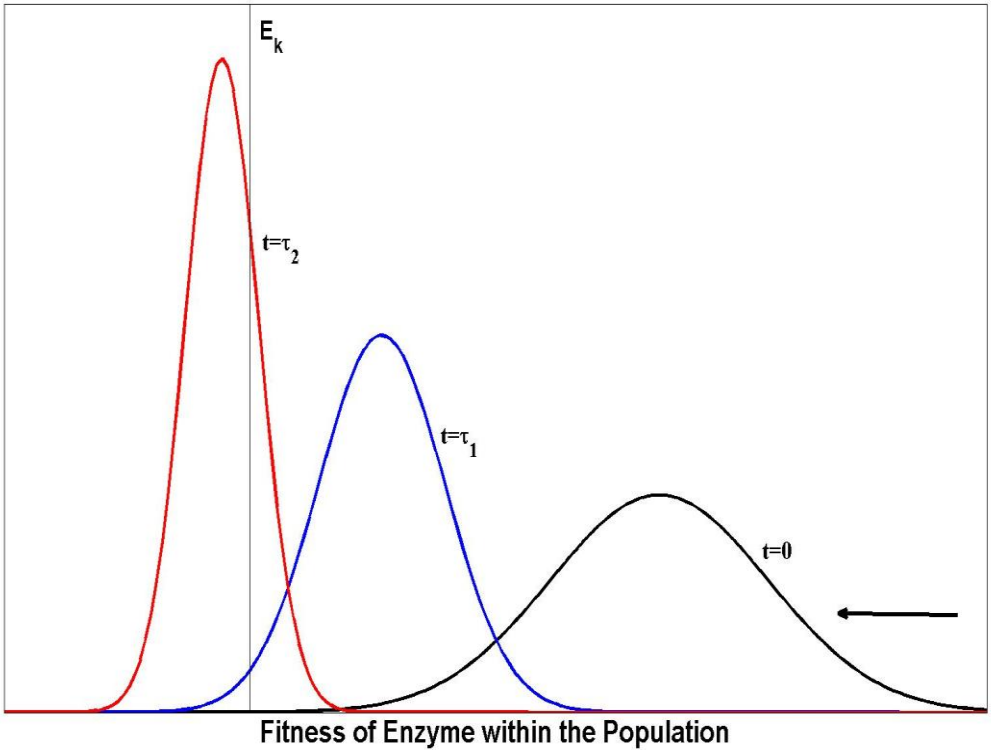

Figure 4.2: Enzyme Fitness Evolution

The probability of kill, P_k, for the spore population is the cumulative probability up to the kill threshold, $\Phi_{E_r(t_e)}(E_k)$, that is

$$\begin{aligned}\Phi_{E_r(t_e)}(E_k) &= P_k(E_r(t_e) < E_k) \\ &= P_k(E_0 f_E(T,t_e) < E_k) \\ &= P_k\left(E_0 < \frac{E_k}{f_E(T,t_e)}\right),\end{aligned}$$

Using equation 4.7,

$$\begin{aligned}P_k(E_0 < \frac{E_k}{f_E(T,t_e)}) &= \frac{1}{\sigma_{E_0}\sqrt{2\pi}} \int_{-\infty}^{\frac{E_k}{f_E(T,t_e)}} e^{-\frac{(E_0-\mu E_0)^2}{2\sigma_{E_0}^2}} dE_0 \\ &= \frac{1}{2}[1+erf(Q_E)]\end{aligned}$$

where

$$Q_E = \frac{E_k - \mu_{E_0} f_E(T, t_e)}{\sigma_{E_0} \sqrt{2} f_E(T, t_e)}.$$

4.3.2 Beta Model.

The Gaussian distribution is often used because the random variables can be standardized, but this assumes the random variables are between negative infinity and positive infinity. However, since the maximum amount of enzymes, E_{max}, within any spore cannot be infinite nor can the minimum amount be negative, the Gaussian representation may not give an adequate physical representation. A probability distribution bounded by [0, E_{max}] would provide a better estimation of the fitness probability. Therefore, the beta distribution which is defined on a positive range and bounded will be used to model the initial enzyme content.

The beta probability density family is represented by a two-parameter density function typically defined over the closed interval between zero and one [12] and is given by

$$f(x) = \begin{cases} \frac{\Gamma(\alpha+\beta)}{\Gamma(\alpha)\Gamma(\beta)} x^{\alpha-1}(1-x)^{\beta-1}, & 0 \le x \le 1,\ \alpha > 0,\ \beta > 0, \\ 0, & x > 1. \end{cases} \tag{4.9}$$

Here $\Gamma(\alpha)$ is the gamma function [12] where

$$\Gamma(\alpha) = \int_0^\infty x^{\alpha-1} e^{-x} dx.$$

Refer to Ref. 12 for additional properties of the gamma function.

The beta cumulative distribution is then

$$P(x \le x_0) = \begin{cases} \dfrac{\Gamma(\alpha+\beta)}{\Gamma(\alpha)\Gamma(\beta)} \int_0^{x_0} x^{\alpha-1}(1-x)^{\beta-1}dx, & 0 \le x_0 \le 1 \\ 1, & x_0 > 1 \end{cases} \tag{4.10}$$

This beta distribution can be expressed in terms of the incomplete beta function [12], $B_{x_0}(\alpha,\beta)$, given by

$$B_{x_0}(\alpha,\beta) = \int_0^{x_0} x^{\alpha-1}(1-x)^{\beta-1}dx. \tag{4.11}$$

Thus,

$$P(x \le x_0) = \begin{cases} \dfrac{\Gamma(\alpha+\beta)}{\Gamma(\alpha)\Gamma(\beta)} B_{x_0}(\alpha,\beta), & 0 \le x_0 \le 1 \\ 1, & x_0 > 1 \end{cases}$$

As noted above, the concentration of each enzyme within the spore is between zero and $E_{max}^{(i)}(T,t_e)$ where $E_{max}^{(i)}(T,t_e) = E_{max_0}^{(i)} f_E(T,t_e)$. $E_{max_0}^{(i)}$ is the maximum concentration of each enzyme prior to any treatment and $f(T,t_e)$ is given in Equation 4.5. By dividing the concentration of each enzyme amount by $E_{max}^{(i)}(T,t_e)$, the concentration of each enzyme will be proportions between zero and one. In order to generate the physically realistic representation of the spore's initial enzyme content, it was assumed that initially $\alpha >> \beta$. From this assumption, the mean amount of enzymes will be close to the maximum possible, E_{max}, and the probability distribution of enzymes will be skewed.

Although, the beta density function is only nonzero on the interval 0 < x < 1, it can be rescaled for an arbitrary finite interval. To this end, set $x = \dfrac{E_r(t_e)}{a}$ where $a = E_{max}(T,t_e)$ and define $E_0 = x_0 a$ in Equation 4.10 to produce

$$P(E_r(t_e) \le E_0) = \begin{cases} \frac{\Gamma(\alpha+\beta)}{\Gamma(\alpha)\Gamma(\beta)} \int_0^{E_0} \left(\frac{E_r(t_e)}{a}\right)^{\alpha-1} \left(1-\frac{E_r(t_e)}{a}\right)^{\beta-1} \frac{dy}{a}, & 0 \le \frac{E_0}{a} \le 1 \\ 1, & \frac{E_0}{a} > 1 \end{cases}$$

$$= \begin{cases} \frac{\Gamma(\alpha+\beta)}{\Gamma(\alpha)\Gamma(\beta)} a^{1-(\alpha+\beta)} \int_0^{E_0} E_r(t_e)^{\alpha-1} (a-E_r(t_e))^{\beta-1} dy, & 0 \le E_0 \le a \\ 1, & E_0 > a \end{cases}$$

This leads to the associated scaled density function

$$f(E_r(t_e)) = \begin{cases} \frac{\Gamma(\alpha+\beta)}{\Gamma(\alpha)\Gamma(\beta)} a^{1-(\alpha+\beta)} E_r(t_e)^{\alpha-1} (a-E_r(t_e))^{\beta-1}, & 0 \le E_r(t_e) \le a \\ 0, & E_r(t_e) > a \end{cases} \quad (4.12)$$

Figure 4.3 shows an illustration of a notional enzyme fitness density function with $\alpha = 10$ and $\beta = 3$ prior to any heat treatment. The random variable, E_0, will be drawn from this enzyme fitness distribution with mean, μ_{E_0} and variance, $\sigma_{E_0}^2$. As exposure time increases, the distribution of the enzymes will evolve. Since E_0 is a random variable, $E_r(t_e)$ is a random variable with mean, μ_{E_r} and variance, $\sigma_{E_r}^2$.

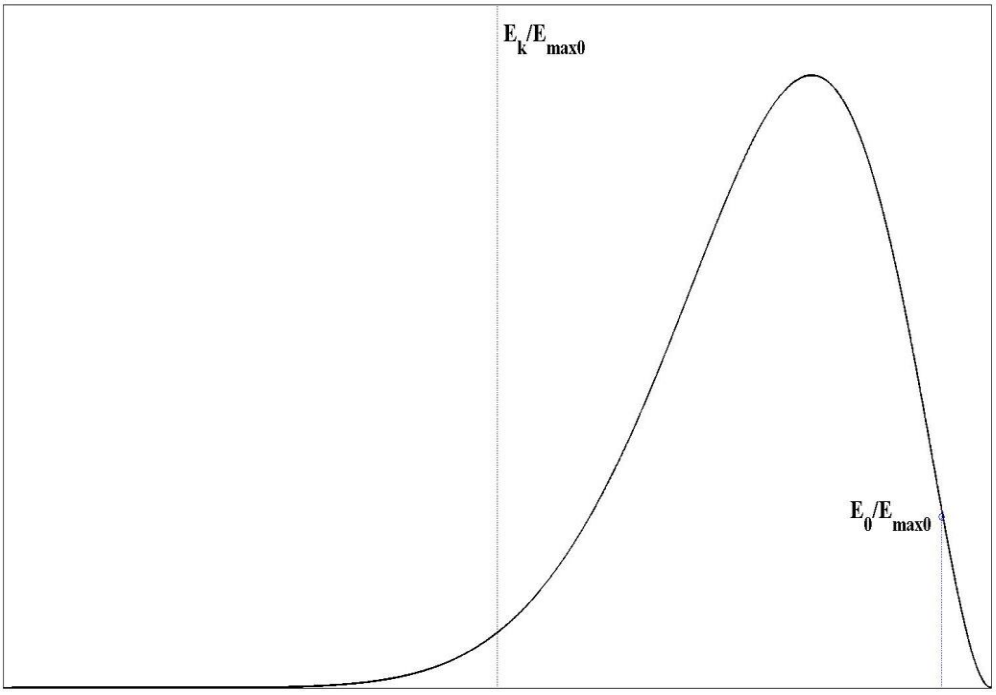

Figure 4.3: Enzyme Fitness Prior to Any Heating (Beta)

Using the expectation rules above,

$$\begin{aligned}\mu_{E_r} &= E\{E_r(t_e)\} \\ &= E\{E_0 f_E(T,t_e)\} \\ &= f_E(T,t_e)E\{E_0\} \\ &= f_E(T,t_e)\mu_{E_0}\end{aligned}$$

and

$$
\begin{aligned}
\sigma_{E_r}^2 &= E\{E_r^2\} - \mu_{E_r}^2, \\
&= E\{E_0^2[f_E(T,t_e)]^2\} - \left(\frac{\alpha}{\alpha+\beta}[f(T,t_e)]^2\right)^2, \\
&= [f_E(T,t_e)]^2\left[E\{E_0^2\} - \left(\frac{\alpha}{\alpha+\beta}\right)^2\right], \\
&= [f_E(T,t_e)]^2\left[\frac{\Gamma(\alpha+\beta)}{\Gamma(\alpha)\Gamma(\beta)}\int_0^1 E_0^2(E_0)^{\alpha-1}(1-E_0)^{\beta-1}dE_0 - \left(\frac{\alpha}{\alpha+\beta}\right)^2\right], \\
&= [f_E(T,t_e)]^2\left[\frac{\Gamma(\alpha+\beta)}{\Gamma(\alpha)\Gamma(\beta)}\int_0^1 (E_0)^{(\alpha+2)-1}(1-E_0)^{\beta-1}dE_0 - \left(\frac{\alpha}{\alpha+\beta}\right)^2\right], \\
&= [f_E(T,t_e)]^2\left[\frac{\Gamma(\alpha+\beta)}{\Gamma(\alpha)\Gamma(\beta)}\frac{\Gamma(\alpha+2)\Gamma(\beta)}{\Gamma(\alpha+2+\beta)} - \left(\frac{\alpha}{\alpha+\beta}\right)^2\right], \\
&= [f_E(T,t_e)]^2\left[\frac{\Gamma(\alpha+1+\beta-1)}{\Gamma(\alpha+1-1)}\frac{\Gamma(\alpha+2)}{\Gamma(\alpha+2+\beta)} - \left(\frac{\alpha}{\alpha+\beta}\right)^2\right].
\end{aligned}
$$

Using, the property that $x\Gamma(x) = \Gamma(x+1)$

$$
\begin{aligned}
\sigma_{E_r}^2 &= [f_E(T,t_e)]^2\left[\frac{\Gamma(\alpha+\beta+1)}{(\alpha+\beta)}\frac{\alpha}{\Gamma(\alpha+1)}\frac{(\alpha+1)\Gamma(\alpha+1)}{(\alpha+\beta+1)\Gamma(\alpha+\beta+1)} - \left(\frac{\alpha}{\alpha+\beta}\right)^2\right], \\
&= [f_E(T,t_e)]^2\left[\frac{\alpha(\alpha+1)}{(\alpha+\beta)(\alpha+\beta+1)} - \left(\frac{\alpha}{\alpha+\beta}\right)^2\right], \\
&= [f_E(T,t_e)]^2\frac{\alpha\beta}{(\alpha+\beta)^2(\alpha+\beta+1)} \\
&= [f_E(T,t_e)]^2\sigma_{E_0}^2
\end{aligned}
$$

As exposure time increases from $t_e = 0$ to $t_e = \tau_2$, $E_r(t_e)$ moves closer to the kill threshold as depicted in Figure 4.4. The curve outlined in blue represents the enzyme distribution at exposure time, $t_e = 0$. Since no enzyme damage has yet occurred, the population mean is 10/13 (for α=10 and β=3). The curve outlined in green represents the enzyme distribution after some enzyme damage at time, $t_e = \tau_1$, $\tau_1 < \tau_2$. Now that damage

has been done to the enzymes, the mean $\mu_{E_r}(\tau_1) < \mu_{E_0}$. The curve outlined in red represents the enzyme distribution at exposure time, $t_e = \tau_2$. Here the spore's enzymes have accumulated even greater damage and the mean $\mu_{E_r}(\tau_2) < \mu_{E_0}$. Also, the majority of the fitness distribution has exceeded the kill threshold and thus, there will be little viable enzymes available for DNA repair process. Possessing behaviors similar to those when using the Gaussian representation, as exposure time increases the mean and variance of the distribution also decreases.

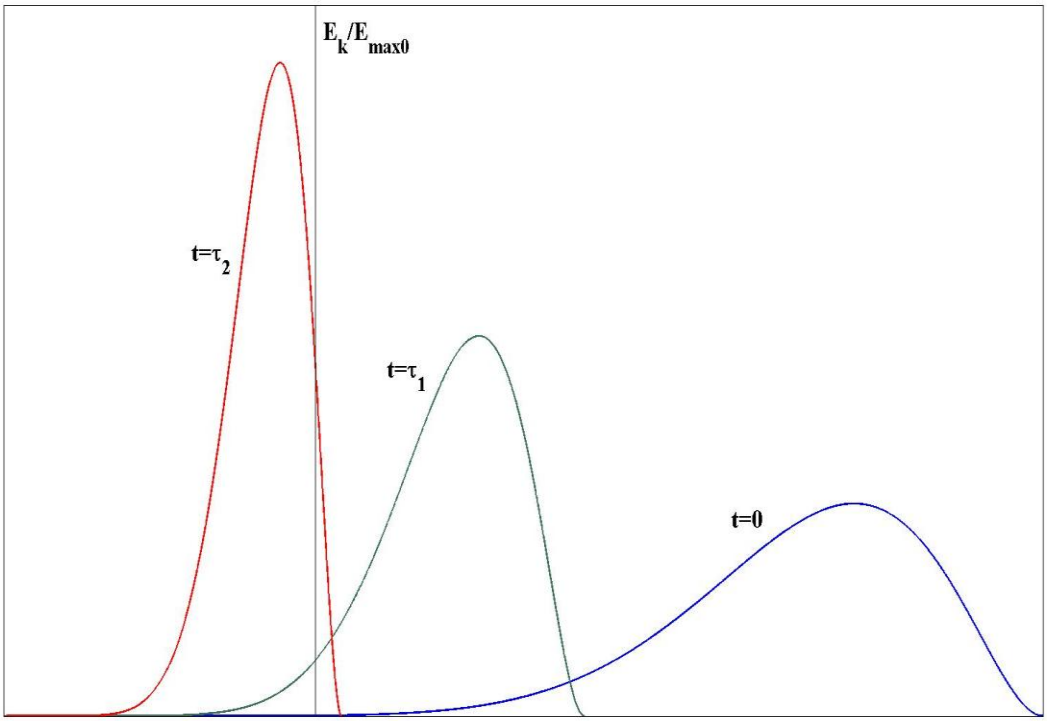

Figure 4.4: Enzyme Fitness Evolution (Beta)

The probability of kill, P_k, can be found by computing the cumulative probability up to the kill threshold. Notationally,

$$P_k\left(\frac{E_r(t_e)}{E_{max}(T,t_e)} < \frac{E_k}{E_{max}(T,t_e)}\right) = P_k\ \ E_0 f(T,t_e) < E_k\ \ ,$$
$$= P_k\ \ E_0 < E_k$$

where $E_k = \frac{E_k}{f(T,t_e)}$.

Then from equation 4.10,

$$P_k(E_0 < E_k) = \begin{cases} \frac{\Gamma(\alpha+\beta)}{\Gamma(\alpha)\Gamma(\beta)} \int_0^{E_k} E_0^{\alpha-1}(1-E_0)^{\beta-1} dE_0, & 0 \le E_k \le 1 \\ 1, & E_k > 1 \end{cases}$$
$$= \begin{cases} \frac{\Gamma(\alpha+\beta)}{\Gamma(\alpha)\Gamma(\beta)} B_{E_k}(\alpha,\beta), & 0 \le E_k \le 1 \\ 1, & E_k > 1 \end{cases}$$

4.3.3 Probability of Survival.

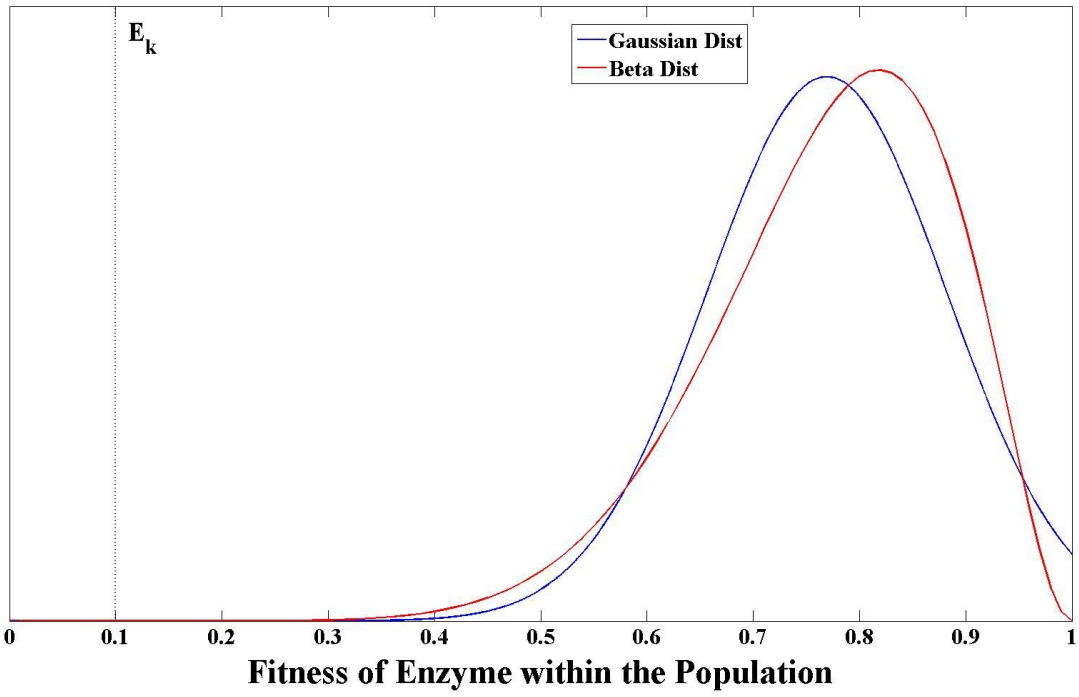

Figure 4.5: Gaussian and Beta Distribution Comparison

Figure 4.5 shows a comparison between the Gaussian and beta density functions prior to any exposure time. In order to make this comparison, the mean and variance were chosen to be the same, that is,

$$\mu_{E_0} \approx 0.7692,$$
$$\sigma_{E_0}^{\ 2} \approx 0.0127.$$

The Gaussian density function exceeds one while the beta density function is bounded by one. This will be the basis for comparing the probability of survival for the Gaussian and beta distribution.

The notional parameters used within the probability of kill models can be found in Table 4.1 [5, 22, 25, 29, 40].

Table 4.1: Parameters for Probability of Kill Models

Parameter	Value	Units
R	1.986×10^{-3}	kcal/mol^{o}K
A_1	4×10^{10}	sec^{-1}
E_1	26.1	kcal/mol
A_2	4.828×10^{15}	sec^{-1}
E_2	38.3	kcal/mol
$\hat{A}_1$	1.6×10^{3}	sec^{-1}
$\hat{E}_1$	10	kcal/mol

Figure 4.6 depicts the probability of enzyme survival during dry heating or $\gamma = 0$ with an initial release temperature of 225^{o}C and a kill threshold of 0.1. That is, once the enzyme population drops to 10%, the spore will not contain the necessary enzyme for DNA repair. The red curve is the beta distribution representation for the fitness model

and blue curve is the Gaussian representation. As it can be seen, the beta representation drops off faster than the Gaussian. This is because the Gaussian distribution is not bounded above like the beta distribution. With the beta representation, it will take about thirty seconds to achieve a significant reduction (10^{-10}) in enzyme survival and for the Gaussian representation, it will take about thirty-six seconds to receive the same reduction.

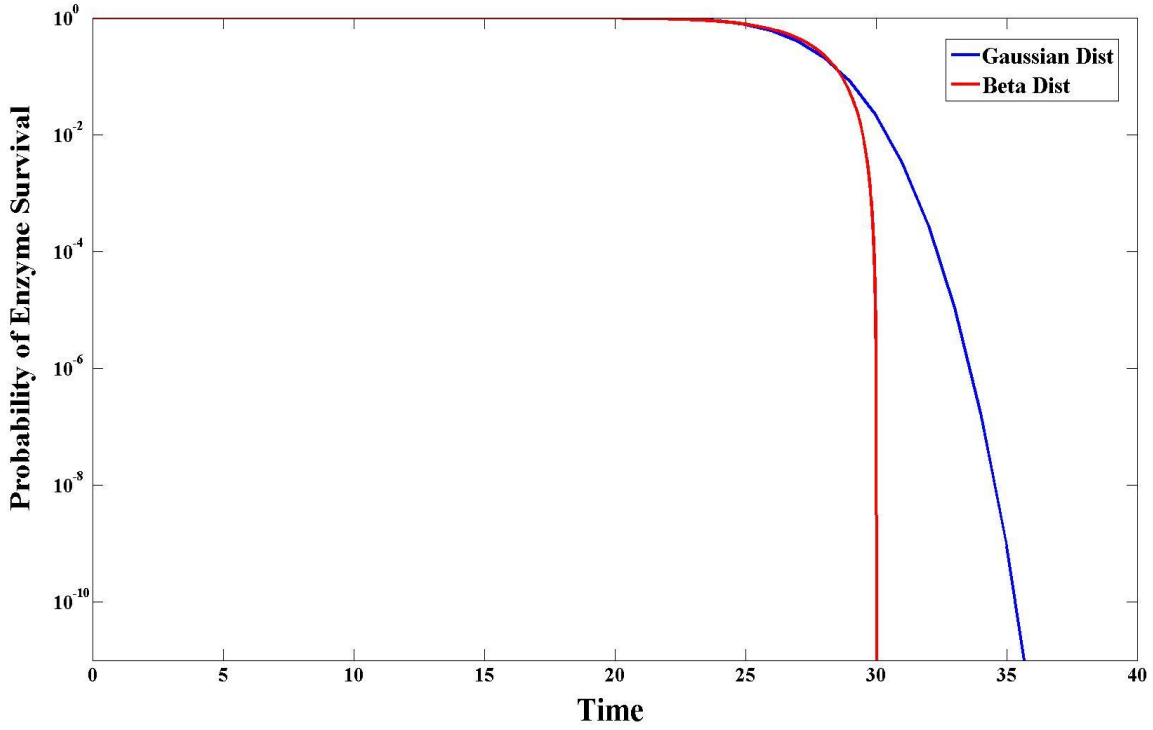

Figure 4.6: Probability of Enzyme Survival (225 C)

Figure 4.7 illustrates the probability of enzyme survival for dry heating with an initial release temperature of 300^{o}C. Again, notice that the estimate of spore survival in the beta model falls of faster than the Gaussian model. When heated at higher temperatures, equivalent enzyme damage takes place within a shorter duration. With the

beta model, it only takes approximately 0.0038 seconds to reduce the enzyme survival by a significant amount. With the Gaussian model, it takes approximately 0.0041 seconds to receive the same reduction. This can be explained by the fact that from Chapter 2 at 290^{o}C, chemically bound water becomes available within the spores. The release of chemically bound water causes the enzymes to be damaged faster as more water is available for hydrolysis reactions.

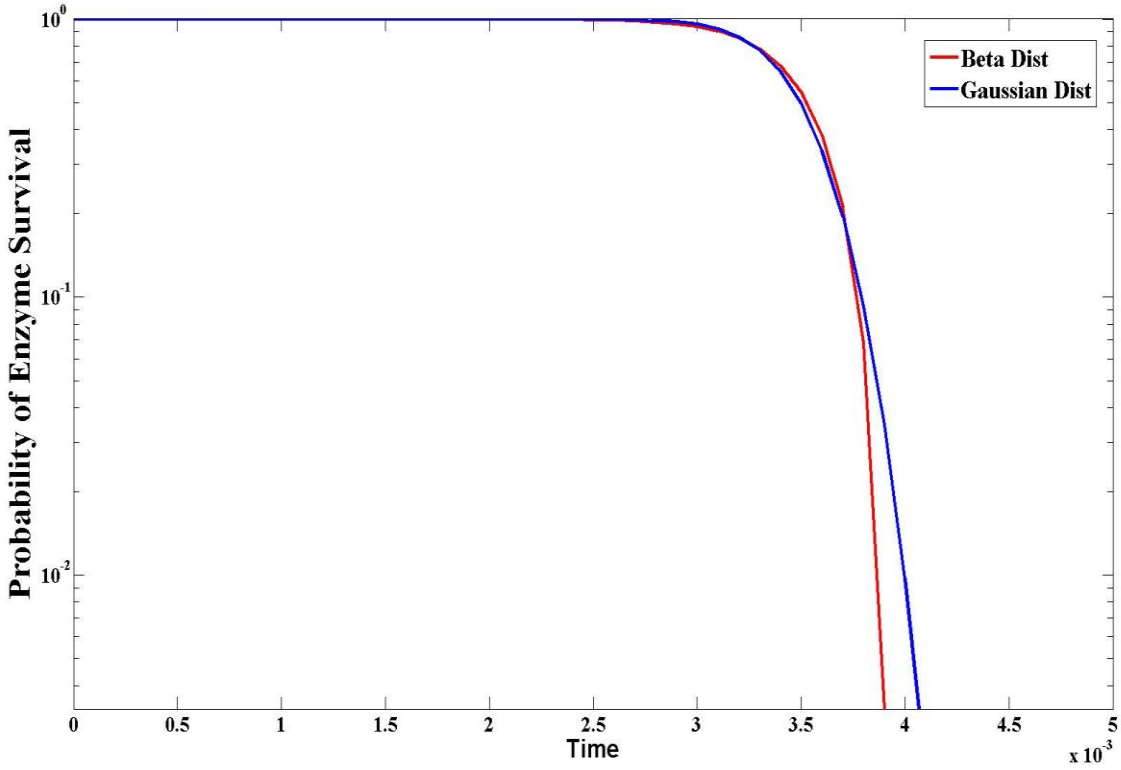

Figure 4.7: Probability of Enzyme Survival (300 C)

5. Germination and Outgrowth

5.1 Introduction

Once the environment becomes nutrient rich, the spore can break the dormant state and move into germination. There are three stages of germination: activation, germination, and outgrowth. During activation, the spore prepares to germinate. During germination, the dormant spore's resistance mechanisms are eliminated and metabolic activity begins as a vegetative cell is formed. Also, during germination, the spore's DNA will be repaired if there are enough viable enzymes for the repair process. If the spore's DNA is repaired, the spore transitions into outgrowth. During outgrowth, the spore's proteins and DNA are synthesized for daughter cells. An initial vegetative cell is first formed from the spore. Whether the spore can survive to the last stage of outgrowth is dependent on several events, such as the exposure time and temperature during thermal inactivation, the initial state of the DNA, as well as the extent of viable enzymes to complete the repair process.

5.2 Germination

Germination is an irreversible and degradative process in which the spore transforms from dormant and highly resistance spore to an actively growing and dividing cell. Many changes occur during germination. The spore' resistance to heat, desiccation, ultraviolet radiation, and chemicals are lost.

Activation reversibly conditions the spore to germinate if appropriate germinants are provided [27]. This process may take less than one minute for an individual spore and

longer for a population of spores. Mild heating of approximately 65^{o}C or the presence of certain chemicals triggers this stage. After activation, "the core enzymes do not function properly and the core water content remains low" [27].

Germination terminates the dormant spore resistance, metabolic inactivity, and refractivity. It occurs when the spore come into contact with many types of nutrients such as amino acids, sugars, and purine nucleosides [33]. The result is the initiation of a breakdown of macromolecules and excretion of spore substances such as the release of the dipicolinic acid, calcium, and peptides [16]. These substances are replaced by water [30]. There are observable physical changes within the layers of the spore structure during this stage. The spore coat remains intact, but the cortex dissolves as the core swells, filling the exosporium. This resulting increase in the spore volume is an important step in the rehydration of the core.

Furthermore, during this stage, the spore's damaged DNA is repaired. As mentioned above, since enzyme synthesis does not occur during dormancy, the spore must contain enough viable enzymes in order to complete the DNA repair process. Additionally, "if too much damage has been accumulated during spore dormancy, this damage can overwhelm the capacity of the repair systems and lead to the death of the germinated spore" [34].

As mentioned in Chapter 4, although there are numerous types of mechanisms to repair damaged DNA, it is believed that BER will mostly likely be necessary within the spore during germination.

5.2.1 DNA BER.

Figure 5.1 illustrates the BER process after U has been formed by deamination of C and is therefore opposite G in the DNA strand. Initially, the bond between uracil and the deoxyribose is cleaved by a DNA glycosylase. This leaves an apurinic/apyrimidinic (AP) site, a sugar with no base attached in the DNA. Next, AP endonuclease cleaves the DNA chain. Deoxyribose phosphodiesterase removes the remaining deoxyribose. The gap is then filled by DNA polymerase and sealed by ligase with the correct base, cytosine.

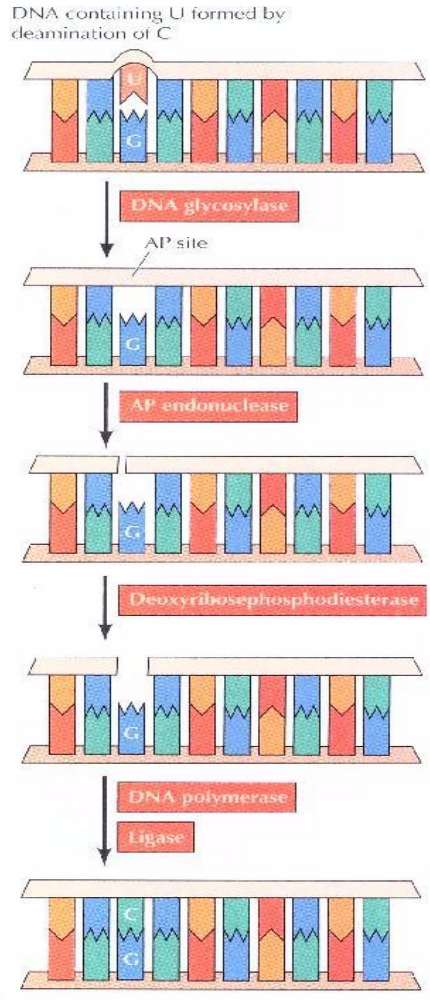

Figure 5.1: Base Excision Repair [3]

Many pathways exist for the BER. Quantitative models exist for this type of repair mechanism [36]. These models were based on Michaelis-Menten kinetics, which is also the foundation of the work in this research

5.2.2 Michaelis-Menten Kinetics

Enzymes act as regulators of biochemical processes such as DNA repair. Enzyme kinetics is the study of the rates of enzyme-catalyzed reactions. Michaelis-Menten kinetics is a model of enzyme kinetics. The Michaelis-Menten equation describes the rates of enzymatic reactions by relating reaction rate to the substrate concentration. The main assumption is that the enzyme and the substrate react reversibly to initially form a complex. The complex then breaks down to form the free enzyme plus one or more products, as shown below,

$$E + S \underset{k_{-1}}{\overset{k_{+1}}{\rightleftharpoons}} ES \xrightarrow{k_{+2}} E + P \tag{5.1}$$

Equation 5.1 states that an enzyme E combines with substrate S to form an ES complex, with a rate constant of k_1. The ES complex then can dissociate to E and S, with a rate constant k_{-1} or it can form a product P, with a rate constant k_2. The turnover number, k_{cat}, is the number of substrate molecules converted into product by an enzyme molecule when the enzyme is fully saturated with substrate and is equal to the rate constant, k_2.

Using Equation 5.1, rate equations can be formed for the concentration of enzyme, substrate, complex, and product, (the notation [ ] represents concentration of)

$$\frac{d[P]}{dt} = k_2[ES], \tag{5.2}$$

$$\frac{d[S]}{dt} = -k_{+1}[E][S] + k_{-1}[ES], \tag{5.3}$$

$$\frac{d[ES]}{dt} = k_{+1}[E][S] - (k_2 + k_{-1})[ES], \tag{5.4}$$

$$\frac{d[E]}{dt} = -k_{+1}[E][S] + (k_2 + k_{-1})[ES], \tag{5.5}$$

where t represents time.

The velocity of the reaction, V, is the rate of product of the concentration of a substrate with the rate coefficient. For example in Equation 5.2, the reaction velocity for [P] is the product of rate constant, k_2, with the concentration of complex, [ES], i.e.

$$V = \frac{d[P]}{dt} = k_2[ES]. \tag{5.6}$$

To solve Equations 5.2-5.6, initial conditions are necessary. If only the enzyme and substrate are present at time t=0, then

$$([S],[E],[ES],[P]) = (S_0, E_0, 0, 0) \tag{5.7}$$

Briggs and Haldane suggested the steady state for the complex is when the concentration of complex stays the same even if the concentrations of starting materials and products are changing. That is, the rate of change in the complex, [ES], is equal to zero, i.e.

$$k_{+1}[E][S] - (k_2 + k_{-1})[ES] = 0.$$

Therefore,

$$\frac{[E][S]}{[ES]} = \frac{(k_2 + k_{-1})}{k_{+1}}. \tag{5.8}$$

Equation 5.8 is the Michaelis constant, K_M,

$$K_M = \frac{(k_2 + k_{-1})}{k_{+1}}. \tag{5.9}$$

The Michaelis constant is independent of enzyme and substrate concentrations. Also, by adding Equations 5.4 and 5.5,

$$\frac{d}{dt}[ES]+[E]=0.$$

This implies that

$$[E]+[ES]=C,$$

where C is a constant. From Equation 5.7, at t=0,

$$[E]+[ES]=E_0 \tag{5.10}$$

Now, by substituting Equation 5.10 into Equation 5.8,

$$[ES]=\frac{(E_0-[ES])[S]}{K_M},$$

and solving for [ES],

$$[ES]=\frac{[S]E_0}{K_M+[S]}. \tag{5.11}$$

Therefore, from Equation 5.6,

$$V=\frac{k_2[S]E_0}{K_M+[S]}. \tag{5.12}$$

This gives the Michaelis-Menten equation. At low substrate concentration, when [S] is much less than K_M,

$$V=\frac{k_2[S]E_0}{K_M}. \tag{5.13}$$

The reaction becomes first order with the rate directly proportional to the substrate concentration. At high substrate concentration, when [S] is much greater than K_M,

$$V=k_2E_0. \tag{5.14}$$

The reaction is now independent of substrate concentration and the rate becomes maximal. The reaction velocity is then said to saturate with respect to the substrate or to

exhibit saturation. Using the Michaelis-Menten theory, quantitative models were developed for the BER of DNA [36]. These models will be further explored in the next section.

5.3 DNA BER Model

Figure 5.2 shows an illustration of a pathway for the BER mechanism with the definitions of substrate concentrations y_i (nM), enzyme concentrations e_i (nM), and reaction velocities v_i (nM/sec).

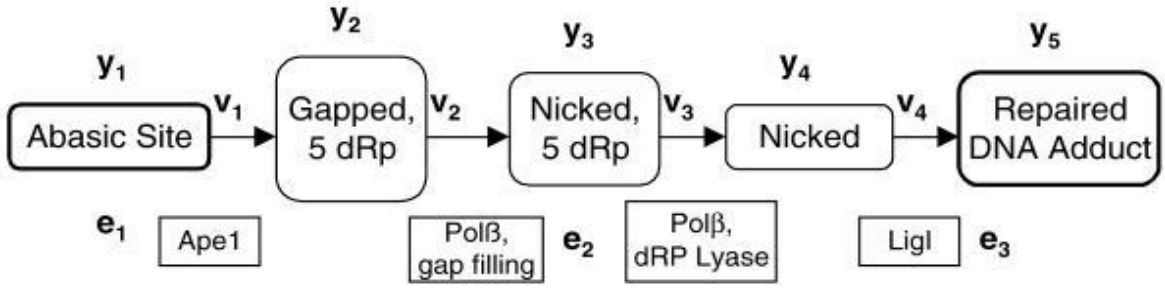

Figure 5.2: Schematic of the DNA Repair Model (BER) [36]

Initially, Ape1 incises the abasic site producing a single nucleotide gap with a 3'-hydroxyl group and a 5'-dRp group. Then, DNA Polβ (e2) fills the gap producing a nicked substrate with a 5'-dRp remaining. The 5'-terminus is then processed by the dRp lyase activity of Polβ. Lastly, DNA ligase (e3) seals the nicked substrate.

A quantitative model of human DNA BER was developed from kinetic data available in by Sokhansanj et al. [36]. By assuming Michaelis-Menten kinetics, the model equations are

$$\frac{dy_1}{dt_r} = -v_1, \qquad v_1 = y_1\left(\frac{k_1 e_1}{y_1 + K_1}\right)$$

$$\frac{dy_2}{dt_r} = v_1 - v_2, \qquad v_2 = y_2\left(\frac{k_2 e_2}{y_2 + K_2}\right)$$

$$\frac{dy_3}{dt_r} = v_2 - v_3, \qquad v_3 = y_3\left(\frac{k_3 e_2}{y_3 + K_3}\right)$$

$$\frac{dy_4}{dt_r} = v_3 - v_4, \qquad v_4 = y_4\left(\frac{k_4 e_3}{y_4 + K_4}\right)$$

$$\frac{dy_5}{dt_r} = v_4.$$

where k (1/sec) represents k_{cat}, K (nM) represents the Michaelis constant, and t_r represents the repair time (sec). Notice that the velocity rates are dependent on the individual enzyme concentrations. Since the enzymes too are damaged during the inactivation process, the amount of viable enzymes is decreased. If the spore contains a sufficient amount of enzymes, then the repair time will be quick. Whereas, if the spore's enzymes are reduced substantially, the repair time will take longer.

Each compartment in Figure 5.2 is dependent on the previous one. If e_1 is reduced during the thermal inactivation, then v_1 would be slow and it will affect the speed of the second compartment, y_2. This in turn would affect the third compartment, y_3. And so on. The same can be same for e_2 and e_3. Reductions in the enzyme concentrations will also affect the repair velocities of each compartment.

This model has been mimicked to explain the repair process within the *Bacillus* spores. Furthermore, this research is interested in DNA information content instead of DNA concentration. Therefore, a dimensionless variable is introduced. Also, from

Chapter 4 since the fitness of each enzyme is assumed to come from a beta distribution, the enzyme concentrations will be scaled by $E_{max}^{(i)}(T,t_e)$. This results in the following

$$\begin{aligned} y_i(t_r) &= \xi_i(t_r) I_0 \\ e_i(T,t_e) &= \gamma_i E_{max}^{(i)}(T,t_e) \end{aligned} \tag{5.15}$$

where $E_{max}^{(i)}(T,t_e)$ represents the maximum enzyme concentration for the ith enzyme type after exposure time. Further, I_0 represents the initial state of the total DNA (critical and non critical) such that

$$I_c = I_0 \theta,$$

and I_c represents the initial state of critical DNA with θ the fraction of the total DNA which is critical. Moreover, the repair process does not recognize the difference between critical and non critical DNA and therefore will repair the total damaged DNA. Substituting the dimensionless variables into the DNA BER model produces five equations as follows

$$\begin{aligned} \frac{d\xi_1(t_r)}{dt_r} &= -\xi_1(t_r)\left(\frac{k_1\gamma_1 E_{max}^{(1)}(T,t_e)}{\xi_1(t_r)I_0 + K_1}\right), \\ \frac{d\xi_2(t_r)}{dt_r} &= \xi_1(t_r)\left(\frac{k_1\gamma_1 E_{max}^{(1)}(T,t_e)}{\xi_1(t_r)I_0 + K_1}\right) - \xi_2(t_r)\left(\frac{k_2\gamma_2 E_{max}^{(2)}(T,t_e)}{\xi_2(t_r)I_0 + K_2}\right), \\ \frac{d\xi_3(t_r)}{dt_r} &= \xi_2(t_r)\left(\frac{k_2\gamma_2 E_{max}^{(2)}(T,t_e)}{\xi_2(t_r)I_0 + K_2}\right) - \xi_3(t_r)\left(\frac{k_3\gamma_2 E_{max}^{(2)}(T,t_e)}{\xi_3(t_r)I_0 + K_3}\right), \\ \frac{d\xi_4(t_r)}{dt_r} &= \xi_3(t_r)\left(\frac{k_3\gamma_2 E_{max}^{(2)}(T,t_e)}{\xi_3(t_r)I_0 + K_3}\right) - \xi_4(t_r)\left(\frac{k_4\gamma_3 E_{max}^{(3)}(T,t_e)}{\xi_4(t_r)I_0 + K_4}\right), \\ \frac{d\xi_5(t_r)}{dt_r} &= \xi_4(t_r)\left(\frac{k_4\gamma_3 E_{max}^{(3)}(T,t_e)}{\xi_4(t_r)I_0 + K_4}\right). \end{aligned} \tag{5.16}$$

In this model, when $\xi_i(t_r)I_0 >> K_i$, the rates become independent of the substrate concentration as in Equation 5.14. When $\xi_i(t_r)I_o << K_i$, the rates become first order linear

equations as in Equation 5.13. The initial concentration of DNA, I_0, plays an important role in the rate equations. To further understand the influences of I_0 on the DNA repair process, a sensitivity analysis was conducted.

5.3.1 Sensitivity Analysis.

Table 5.1 contains the values for parameters used within the original DNA BER model [36].

Table 5.1: Parameters for Model

Parameter	**Value**		**Parameter**	**Value**
k_1	0.625 sec^{-1}		K_1	300 nM
k_2	0.04 sec^{-1}		K_2	100 nM
k_3	0.78 sec^{-1}		K_3	39 nM
k_4	0.05 sec^{-1}		K_4	130 nM

Additionally, from Chapter 4 the DNA information content and enzymes diminishes exponentially from hydrolysis and pyrolysis damage, i.e., recall

$$I_D(t_e) = I_c f_D(T, t_e),$$
$$E_r(t_e) = E_0 f_E(T, t_e).$$

If the rate coefficients associated with pyrolysis and hydrolysis for both DNA information content and enzymes are the same, then the spore's DNA and enzymes will be reduced at the same rate. For example by this simplification, after the inactivation process, if 10% of the spore's DNA is damaged then 10% of the spore's enzymes are also damaged.

An additional assumption must be made about the maximum enzyme concentration for each enzyme prior to thermal heating. The spore contains an initial concentration of enzymes used for the repair process. These initial maximum concentrations are presented in Table 5.2. These values were chosen based on the parameter values in Ref. 33, an exposure time of 2 seconds, and temperature of 300°C.

Table 5.2: Enzyme Maximum Parameters

Enzyme	$E_{max_0}^{(i)}$	$E_{max}^{(i)}(T,t_e)$
1(Ape1)	130 nM	83.19 nM
2 (Polβ)	50 nM	32.00 nM
3 (Ligl)	150 nM	95.99 nM

Multiple cases were examined. Case 1 assumed $\xi(t_r)I_o << K_i$ for all $i = 1,...,4.$ Case 2 assumed $\xi(t_r)I_o \approx K_i$ for some $i = 1,...,4.$ Case 3 assumed $\xi(t_r)I_o >> K_i$ for all $i = 1,...,4.$ The initial DNA information parameter, I_0, for each of these cases is given in Table 5.3,

Table 5.3: I_0 values for Cases 1, 2, 3

Case	I_0
1	10 nM
2	100 nM
3	1000 nM

Further, three levels of damaged DNA and enzymes were considered. These were when 10%, 50%, and 90% of DNA and enzymes are damaged during the thermal heating. Figure 5.3 illustrates the repair of DNA when 10% of the spore's DNA and enzymes are damaged. In this instance, there is little difference between I_0 = 10 nM and I_0 = 100 nM. However, for I_0 = 1000 nM, the rate of repair decreases and it takes longer to repair the damaged DNA. For example, it takes approximately 100 seconds to repair half of the damaged DNA when $I_0 = 10\,nM$ and approximately 146 seconds when I_0 = 1000 nM.

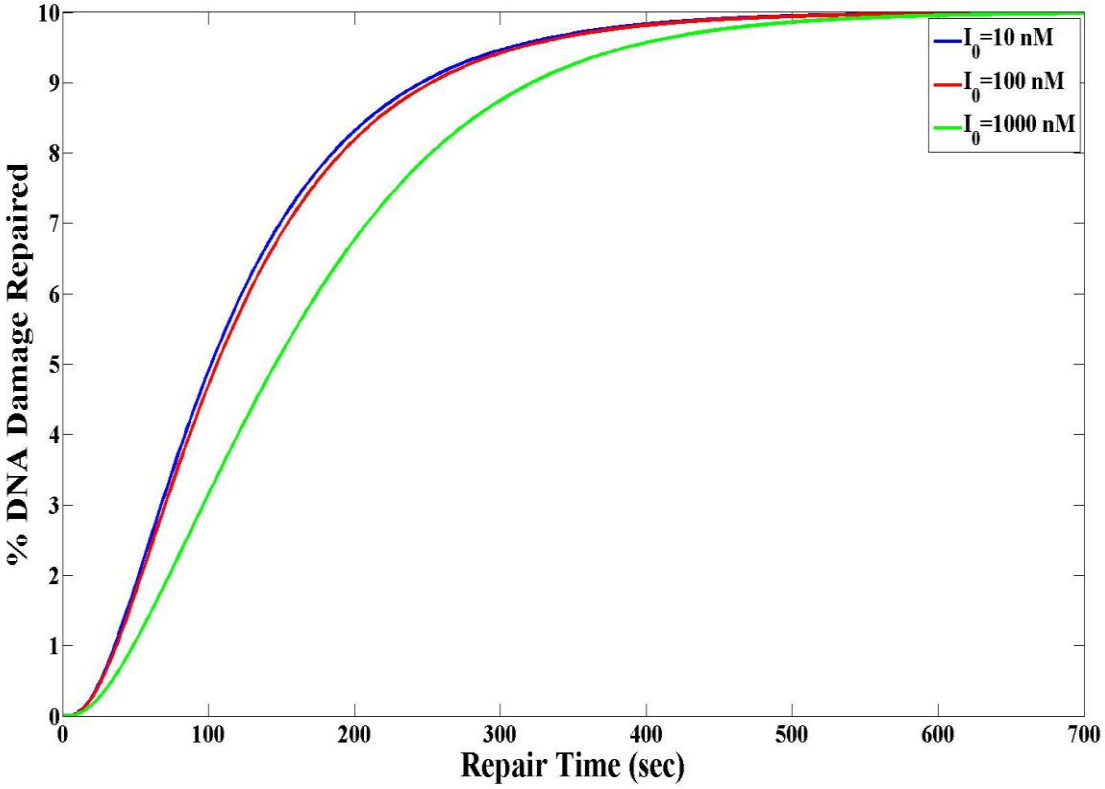

Figure 5.3: DNA Repair Analysis when 10% of DNA & Enzymes are Damaged

Figure 5.4 depicts the repair of DNA when 50% of the spore's DNA and enzymes have been damaged. Compared to Figure 5.3, the repair time has increased because lower

enzymes concentrations are now available for the repair process. Again, when I_0 = 10 nM and I_0 = 100 nM, there is not great difference in the time required to repair the damaged DNA. It takes about 187 seconds when $I_0 = 10$ nM and about 223 seconds when I_0 = 100 nM to repair half of the damaged DNA. Whereas, for I_0 = 1000 nM, it takes approximately 580 seconds to repair half of the damaged DNA.

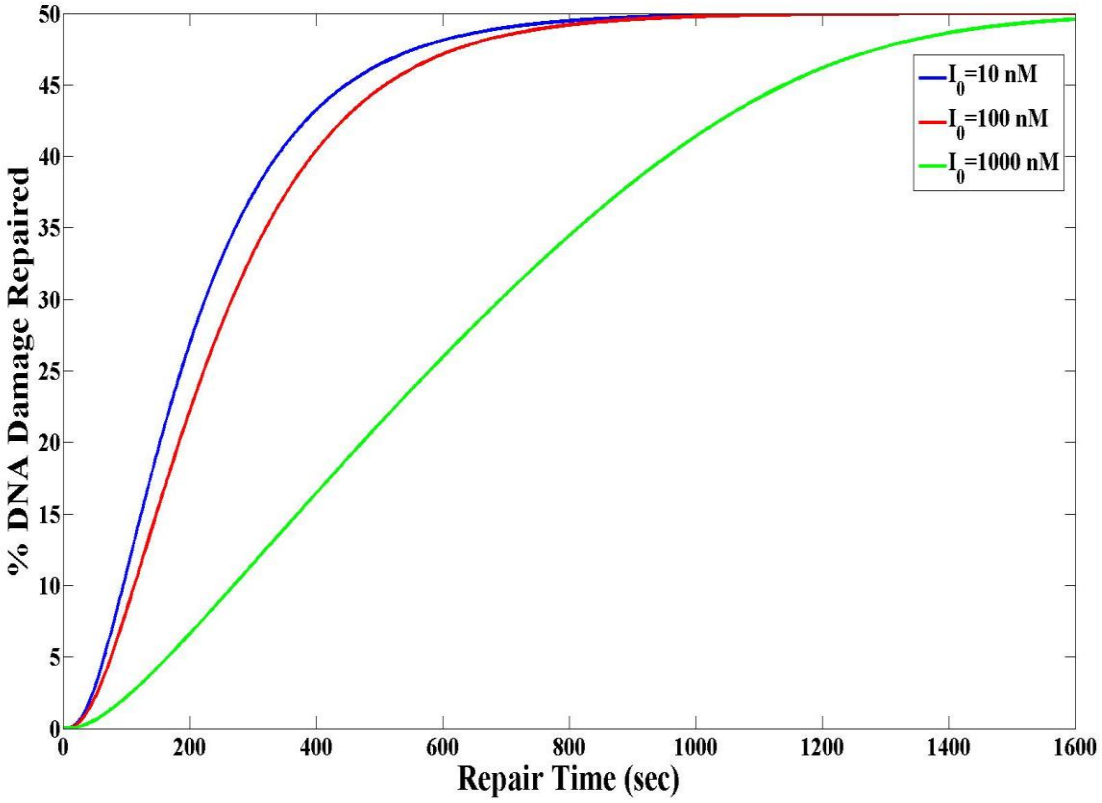

Figure 5.4: DNA Repair Analysis when 50% of DNA & Enzymes are Damaged

Figure 5.5 illustrates the repair of DNA when 90% of the spore's DNA and enzymes have been damaged. When the majority of the spore's enzymes are damaged, the repair process takes much longer than in the previous cases. In order to repair half of

the damaged DNA when I_0 = 1000 nM , the time required would be 4477 seconds or roughly 1 hour and 14 minutes.

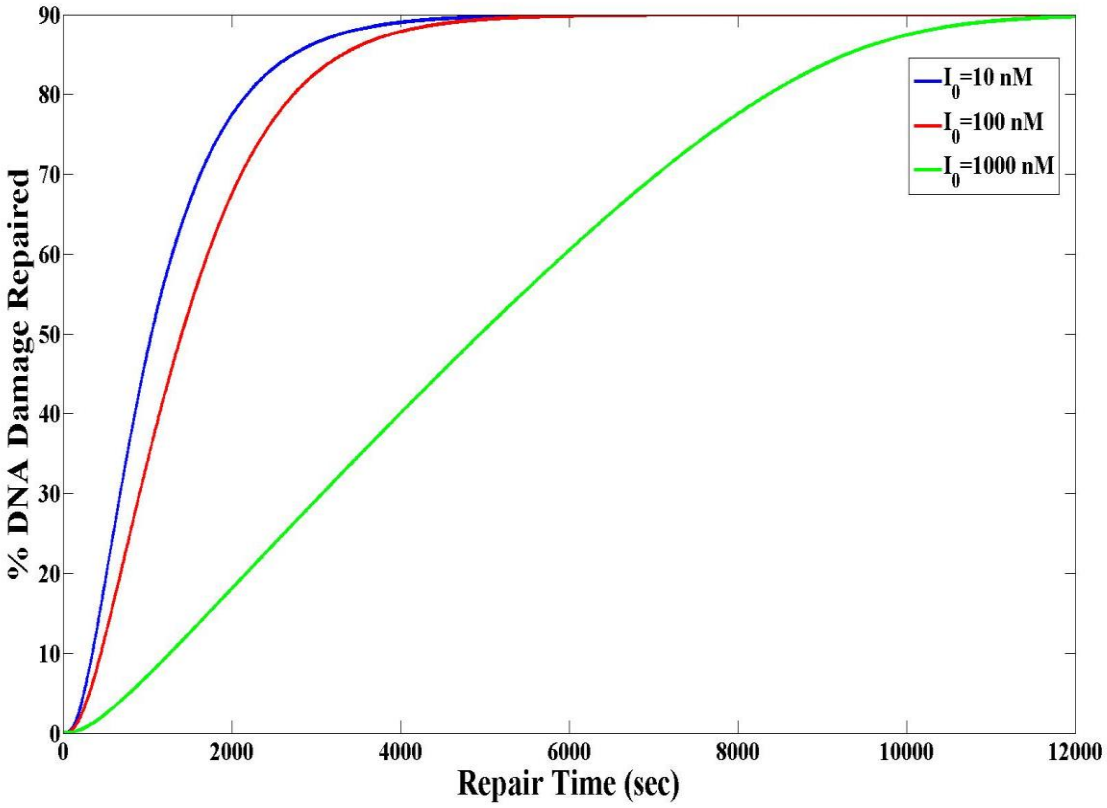

Figure 5.5: DNA Repair Analysis when 90% of DNA & Enzymes are Damaged

Thus, the initial state of DNA is important in the repair rate and whether or not the spore will be able to repair the damaged DNA. If Case 1 holds true, then the DNA BER model becomes a system of first order linear equations. Therefore, an analytical solution can be written. The influence that assumption has on the DNA BER model will be examined in the next section.

5.3.2 Linear Model of DNA BER Model.

When $\xi(t_r)I_o \ll K_i$, the substrates stay far from saturation where a saturation value will be defined as $\frac{K_i}{I_0}$. The DNA BER model equations can be reduced to a first order linear system. Assume that $\xi(t_r)I_o \ll K_i$ for i=1,…,4. The influence of the enzymes and initial state of DNA will be explored.

To linearize the nonlinear model in Equation 5.16, the Taylor series expansion of functions was used. Let $f_i(\xi)$ be a function such that $f_i(0)=0$ and define the differential $\dot{\xi}(t_r) = f_i(\xi(t_r))$. If $\xi(0)=0$, $f_i(\xi)$ may be expanded in a Taylor series about zero to produce

$$f_i(\xi) = f_i(\xi(0)) + \nabla f_i(\xi(0)) \cdot (\xi - \xi(0)) + O((\xi - \xi(0))^2), \qquad i = 1,...,4.$$

Then since $f_i(\xi(0)) = f_i(0) = 0$,

$$f_i(\xi) \approx \nabla f_i(0) \cdot \xi + O(\xi^2), \qquad i = 1,...,4.$$

Using Equation 5.16, the following is obtained

$$\nabla f_1(\xi)|_{\xi=0} = \left\{ -\frac{k_1\gamma_1 E_{max}^{(1)}}{K_1}, 0, 0, 0 \right\},$$
$$\nabla f_2(\xi)|_{\xi=0} = \left\{ \frac{k_1\gamma_1 E_{max}^{(1)}}{K_1}, -\frac{k_2\gamma_2 E_{max}^{(2)}}{K_2}, 0, 0 \right\},$$
$$\nabla f_3(\xi)|_{\xi=0} = \left\{ 0, \frac{k_2\gamma_2 E_{max}^{(2)}}{K_2}, -\frac{k_3\gamma_2 E_{max}^{(2)}}{K_3}, 0 \right\},$$
$$\nabla f_4(\xi)|_{\xi=0} = \left\{ 0, 0, \frac{k_3\gamma_2 E_{max}^{(2)}}{K_3}, -\frac{k_4\gamma_3 E_{max}^{(3)}}{K_4} \right\}.$$

In these results the exposure time and temperature dependence on $E_{max}^{(i)}(T, t_e)$ has been suppressed.

For simplicity, let

$$\lambda_1 = \frac{k_1\gamma_1 E_{max}^{(1)}}{K_1}, \lambda_2 = \frac{k_2\gamma_2 E_{max}^{(2)}}{K_2}, \lambda_3 = \frac{k_3\gamma_2 E_{max}^{(2)}}{K_3}, \lambda_4 = \frac{k_4\gamma_3 E_{max}^{(3)}}{K_4}. \qquad (5.17)$$

Then the Jacobian for the system becomes

$$J = \begin{bmatrix} -\lambda_1 & 0 & 0 & 0 \\ \lambda_1 & -\lambda_2 & 0 & 0 \\ 0 & \lambda_2 & -\lambda_3 & 0 \\ 0 & 0 & \lambda_3 & -\lambda_4 \end{bmatrix}.$$

Thus, $\dot{\xi}(t_r) = J\xi(t_r)$. Therefore, a simple solution can be given as $\xi(t_r) = e^{Jt_r}\xi_0$. Since J is a constant matrix, $\{-\lambda_i\}_{i=1}^4$ are distinct eigenvalues of J with corresponding eigenvectors $\{\zeta_k\}_{k=1}^4$ the solution can be given as

$$\xi_i(t_r) = \sum_{k=1}^{4} c_k^{(i)} \zeta_k^{(i)} e^{-\lambda_k t_r}, \quad i = 1,...,4$$

with

$$\xi(0) = \xi_0 = \sum_{k=1}^{4} c_k \zeta_k = Z e$$
$$\Rightarrow e = Z^{-1}\xi_0$$

where Z is the matrix of eigenvectors,

$$Z = [\zeta_1, \zeta_2, \zeta_3, \zeta_4].$$

The eigenvalues of J are $-\lambda_1, -\lambda_2, -\lambda_3, -\lambda_4$ with corresponding eigenvectors,

$$\zeta_1 = \left[1, -\frac{\lambda_1}{\lambda_1 - \lambda_2}, \frac{\lambda_1}{\lambda_1 - \lambda_2}\cdot\frac{\lambda_2}{\lambda_1 - \lambda_3}, -\frac{\lambda_1}{\lambda_1 - \lambda_2}\cdot\frac{\lambda_2}{\lambda_1 - \lambda_3}\cdot\frac{\lambda_3}{\lambda_1 - \lambda_4}\right]^T,$$

$$\zeta_2 = \left[0, 1, -\frac{\lambda_2}{\lambda_2 - \lambda_3}, \frac{\lambda_2}{\lambda_2 - \lambda_3}\cdot\frac{\lambda_3}{\lambda_2 - \lambda_4}\right]^T,$$

$$\zeta_3 = \left[0,\ 0,\ 1,\ -\frac{\lambda_3}{\lambda_3 - \lambda_4}\right]^T,$$

$$\zeta_4 = 0,\ 0,\ 0,\ 1^T.$$

Figure 5.6 shows comparisons between the numerical solution of the nonlinear DNA BER model equations and the linearization solution if 50% of the spore DNA and enzymes are damaged and I_0=10 nM. Values from Tables 5.1-5.2 were used with an exposure time of 2 seconds at a temperature of 300°C. For ξ_1 and ξ_2, there is no distinction between the linear and nonlinear equations. For ξ_3 and ξ_4 , the linear and nonlinear equations reach different peaks and as time progresses they evolve together. Given the Michaelis constant, K_i, in Table 5.1 and I_0 = 10 nM, the saturation value for ξ_1, ξ_2, ξ_3, ξ_4 respectively are 30, 10, 3.9, and 13. Shown in Figure 5.6, each ξ_i stays far from its respective saturation value.

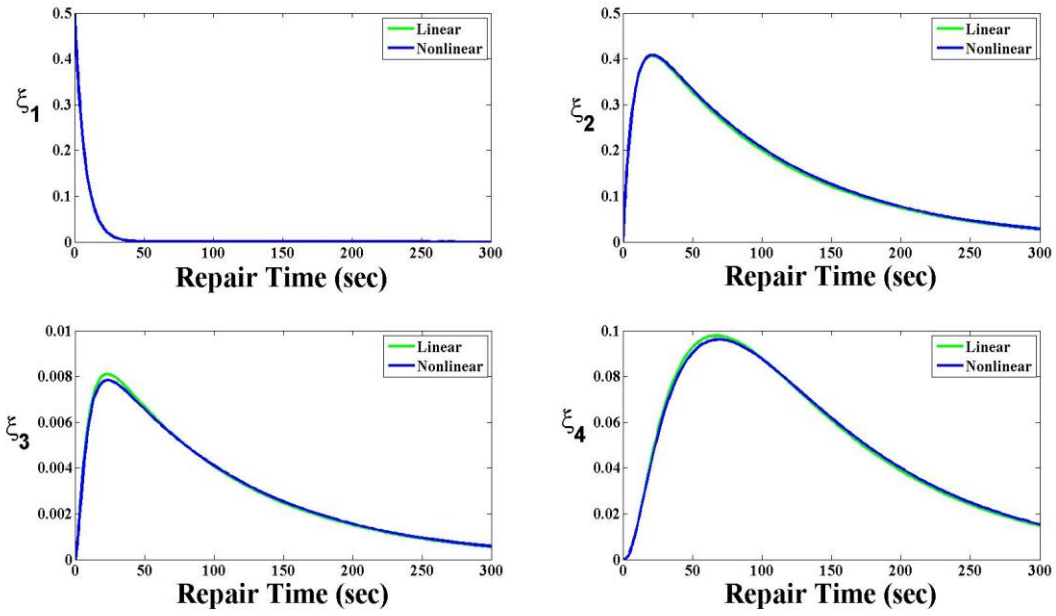

Figure 5.6: Nonlinear and Linear Model Comparison (I_0=10 nM)

Figure 5.7 shows comparisons between the nonlinear DNA BER model and the linear model when I_0=100 nM and 50% of the spore DNA and enzymes are damaged. For ξ_1, there is again no distinction between the linear and nonlinear model equations. For ξ_2, as exposure time progress there is some difference between the nonlinear and linear equations. For ξ_3 and ξ_4 , the linear and nonlinear equations reach different peaks but this difference is not significant since the scaling is small. Further, as repair time progresses, the linear and nonlinear equations evolve together. Here the saturation values for ξ_1, ξ_2, ξ_3, ξ_4 respectively are 3, 1, 0.39, and 1.3. Each ξ_i stays away from its respective saturation value.

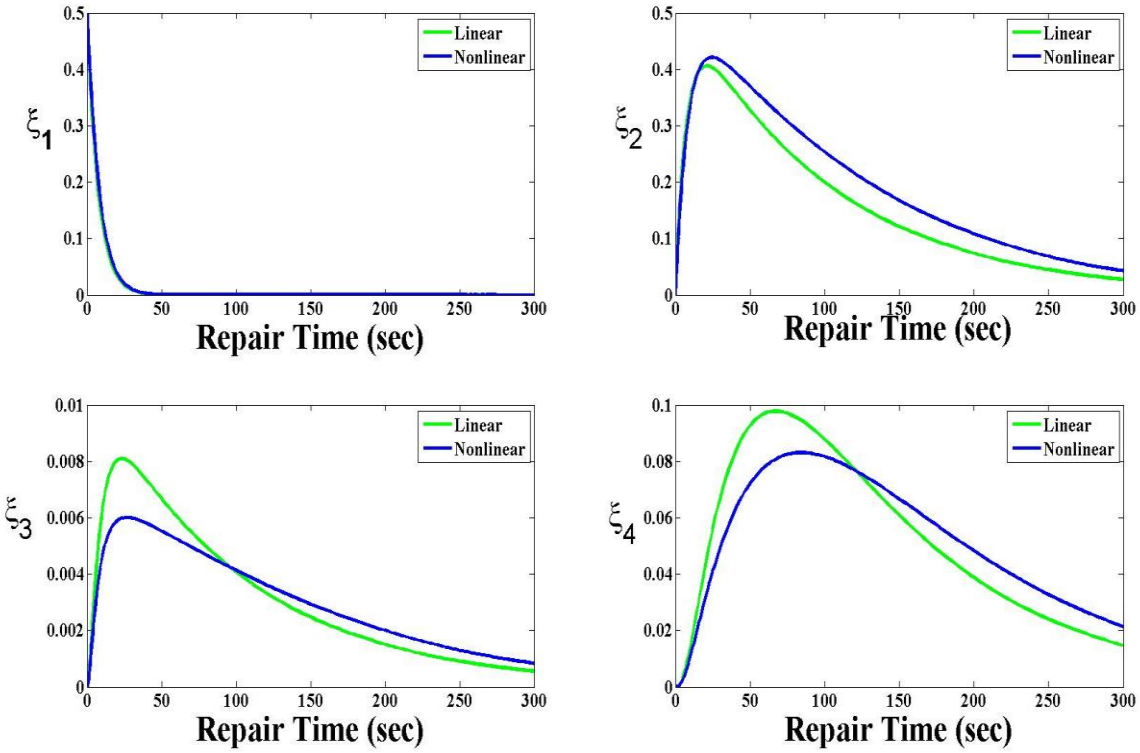

Figure 5.7: Nonlinear and Linear Model Comparison (I_0=100 nM)

Figure 5.8 shows comparisons between the nonlinear DNA BER model and the linear model when I_0=1000 nM and 50% of the spore DNA and enzymes are damaged. For ξ_1, early on there is a difference between the linear and nonlinear model equations but as repair time progress, they evolve together. For ξ_2, the linear and nonlinear equations reach different peaks and as exposure time progress there is some difference between the two. For ξ_3 and ξ_4 , the linear and nonlinear equations reach different peaks. There is also a point at which the nonlinear equations remain constant and therefore, the nonlinear and linear equations do not evolve together. When I_0=1000 nM, the saturation values for ξ_1, ξ_2, ξ_3, ξ_4 respectively are 0.3, 0.1, 0.039, and 0.13. For ξ_1 and ξ_2, each passes their respective saturation value. For ξ_3, the saturation value is not reach and for ξ_4, the saturation value is approached.

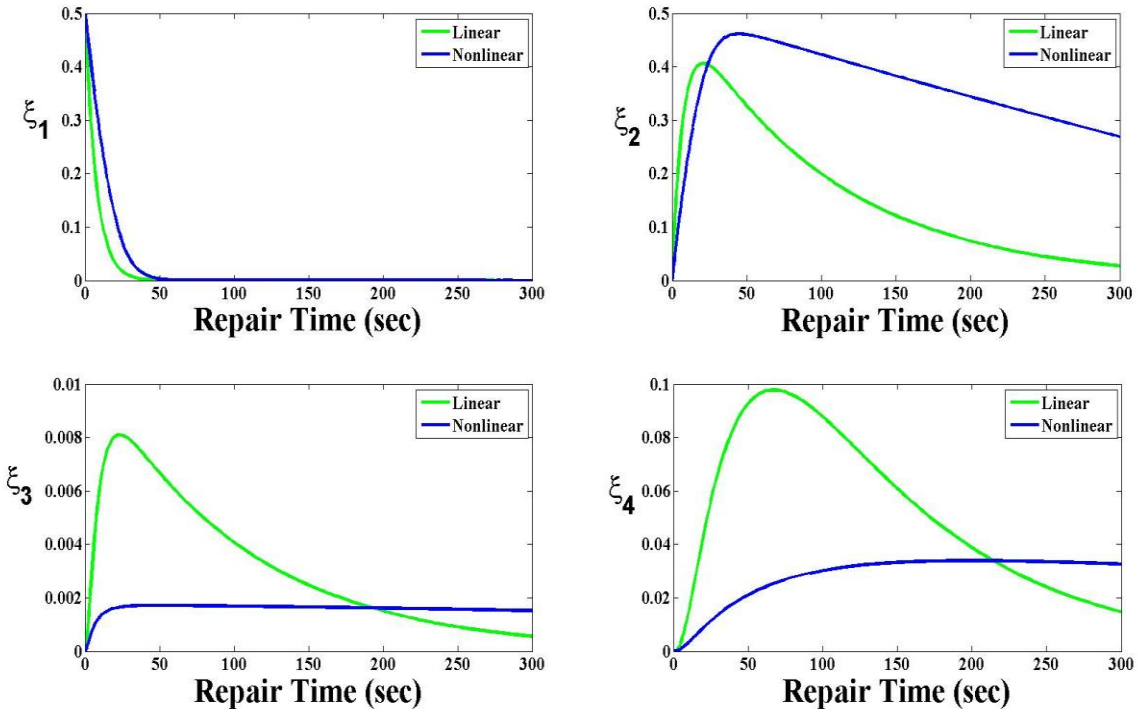

Figure 5.8: Nonlinear and Linear Model Comparison (I_0=1000 nM)

The repair term in the DNA repair model can be given as

$$\xi_5(t_r) = \frac{1}{I_0}\int_0^{t_r} \xi_4(\tau) I_0 \left(\frac{k_4 \gamma_3 E_{max}^3}{K_4 + \xi_4(\tau) I_0} \right) d\tau,$$
$$= \int_0^{t_r} \xi_4(\tau) \left(\frac{k_4 \gamma_3 E_{max}^3}{K_4 + \xi_4(\tau) I_0} \right) d\tau.$$

Assume $\xi_4(t_r) I_o << K_4$, then

$$\xi_5(t_r) = \frac{k_4 \gamma_3 E_{max}^3}{K_4} \int_0^{t_r} \xi_4(\tau) d\tau. \tag{5.18}$$

Evaluating the integral in Equation 5.18 produces

$$\xi_5(t_r;\gamma) = \xi_0^{(4)} \lambda_4 \left\{ \epsilon_1 \left[\frac{1}{\lambda_1} 1 - e^{-\lambda_1 t_r} + \frac{1}{\lambda_4} 1 - e^{-\lambda_4 t_r} \right] + \frac{\epsilon_2}{\lambda_2} 1 - e^{-\lambda_2 t_r} + \frac{\epsilon_3}{\lambda_3} 1 - e^{-\lambda_3 t_r} \right\} \tag{5.19}$$

where

$$\epsilon_1 = \frac{\lambda_1}{\lambda_1 - \lambda_2} \frac{\lambda_2}{\lambda_1 - \lambda_3} \frac{\lambda_3}{\lambda_1 - \lambda_4},$$
$$\epsilon_2 = \frac{\lambda_1}{\lambda_1 - \lambda_2} \frac{\lambda_2}{\lambda_2 - \lambda_3} \frac{\lambda_3}{\lambda_2 - \lambda_4},$$
$$\epsilon_3 = \frac{\lambda_1}{\lambda_1 - \lambda_2} \frac{\lambda_2}{\lambda_1 - \lambda_3} \frac{\lambda_3}{\lambda_3 - \lambda_4}.$$

Observe that under the assumption each enzyme is subjected to the same rate of hydrolysis and pyrolysis reactions, $f_E(T,t_e)$ can be factored with respect to λ resulting in the exposure time appearing only in the exponential terms in Equation 5.19. Therefore, the effect of exposure time will only change the rate at which the velocity equilibrates.

If the spore's DNA is repaired without complications, the next step in germination is outgrowth.

5.4 Outgrowth

Outgrowth is the development of a vegetative cell from a germinated spore [17]. Outgrowth is dependent on the repair of the protein-synthesizing system and an ordered synthesis of proteins [21]. According to Hansen et al, the synthesis of RNA begins after germination and then the proteins are synthesized when the new vegetative cell emerges and divides and outgrowth can last for hours in one spore, but in a population of spores, it occurs synchronously [17]. Let outgrowth time, t_o, be defined as the time when the experimental data is taken to determine if the spore produced a viable cell.

During outgrowth, the core wall thickens to become the vegetative cell wall. Remains of the outer part of the old spore coat and the exosporium are found within the new vegetative cell [16]. Also, in the vegetative cell, "the heat resistance is increased and hardiness is gone" [39]. Figure 5.9 illustrates the vegetative cells forming from the spores.

The spore's chance of survival is dependent on numerous environmental parameters. The probability of survival models examined in Chapter 4 was based on knowledge of a critical threshold for the enzymes. In Figures 4.6 and 4.7, this threshold was chosen to be 0.1. That is, once the enzyme population drops to 10%, the spore will not contain the necessary enzyme for DNA repair. However, this threshold is not a known quantity. In fact, if no DNA damage occurs, no repair enzymes are necessary for outgrowth. Thus, the enzyme threshold may also depend on DNA damage. The influence that the DNA threshold, outgrowth time, and viable enzymes have on the spore's probability of survival will be examined in the following section.

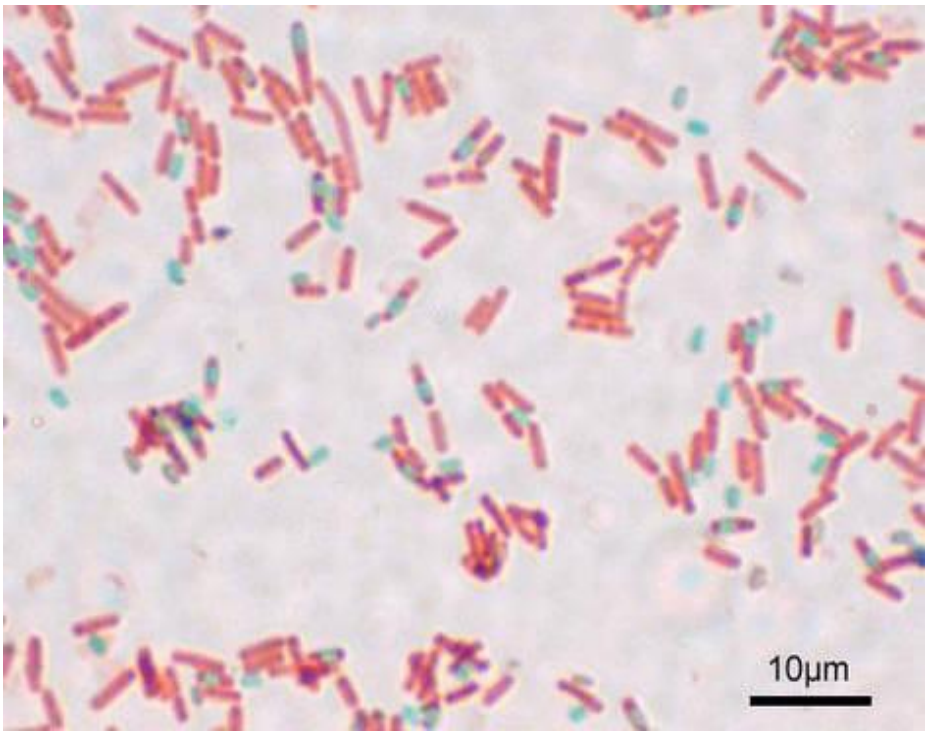

Figure 5.9: Illustration of *Bacillus subtilis* Vegetative Cells [9]

The image is of a stained preparation of *Bacillus subtilis* showing endospores as green and the vegetative cell as red.

5.5 Probability of Survival

5.5.1 Multivariate Probability Distribution.

Let Y_1, Y_2, ..., Y_n be continuous random variables with joint cumulative distribution function $F(y_1, y_2, ..., y_n)$. That is,

$$F(y_1, y_2, ..., y_n) = \int_{-\infty}^{y_1} \int_{-\infty}^{y_2} \cdots \int_{-\infty}^{y_n} f(t_1, t_2, ..., t_n) dt_n \ldots dt_1 \qquad (5.20)$$

where the function $f(y_1, y_2, ..., y_n)$ is the joint probability density function [12].

If Y_1, Y_2, ..., Y_n are independent then

$$F(y_1, y_2, ..., y_n) = F_1(y_1) F_2(y_2) \ldots F_n(y_n)$$

and the joint density function becomes

$$f(y_1, y_2, ..., y_n) = f_1(y_1) f_2(y_2) .. f_n(y_n)$$ [12].

Using these concepts, the probability of survival model based only on single DNA threshold will be derived.

5.5.2 Enzyme Dependence.

The spore's chance of survival is dependent on the available viable enzymes for the DNA repair process. Therefore, the total number of possible combinations of each enzyme, e_1, e_2, and e_3 will determine the domain in which the spore has a chance of survival. Assuming these enzymes are independent random variables, the probability of kill is defined as

$$P_k \; y_5 \; t_r, e \; + \bar{I}_D(T, t_e) < y_c \; = \iiint_D \prod_{i=1}^{3} f_i(e_i) \, de_i, \tag{5.21}$$

where $\bar{I}_D \; T, t_e$ is the fraction of the total undamaged DNA after some exposure temperature and time. This value is computed from Equation 4.2 with

$$\bar{I}_D(T, t_e) = \frac{I_D(T, t_e)}{\theta}.$$

Further, y_5 is the concentration of damaged total DNA which has been repaired after time t_r, and y_c is the critical threshold value below which outgrowth cannot occur. The domain of integration D is defined by

$$D = \{(e_1, e_2, e_3) : y_5(t_r, e) + \bar{I}_D(T, t_e) < y_c\}$$

and $f_i(e_i)$ is the probability density function for fitness due to enzyme e_i, that is

$$f_i(e_i) = \begin{cases} \frac{\Gamma(\alpha+\beta)}{\Gamma(\alpha)\Gamma(\beta)} a^{1-(\alpha+\beta)} e_i^{\alpha-1} (a - e_i)^{\beta-1}, & 0 \le e_i \le a \\ 0, & e_i > a \end{cases} \tag{5.22}$$

where $a = E_{max}^{(i)}(T, t_e)$. Now introducing the dimensionless variables $\xi_i = \frac{y_i}{I_o}$ and $\gamma_i = \frac{e_i}{a}$ from Section 5.4 into Equation 5.21 yields

$$P_k\ \xi_5(t_r, \gamma) + f_D(T, t_e) < \xi_c\ = \int\int\int_D \prod_{i=1}^{3} f_i\ \gamma_i\ \ \frac{d\gamma_i}{a},$$

with

$$f_i(\gamma_i) = \begin{cases} \frac{\Gamma(\alpha+\beta)}{\Gamma(\alpha)\Gamma(\beta)} \frac{1}{a} \gamma_i^{\alpha-1}(1-\gamma_i)^{\beta-1}, & 0 \le \gamma_i \le 1 \\ 0, & \gamma_i > 1 \end{cases}$$

$$D = \{(\gamma_1, \gamma_2, \gamma_3) : \xi_5(t_r, \gamma) + f_D(T, t_e) < \xi_c\},$$

ξ_5 represents the percentage of damaged DNA repaired, ξ_c represents the critical DNA threshold as a percentage of the total repaired, and $f_D(T,t_e)$ is given in Equation 4.2.

Figure 5.10 illustrates the DNA repair for various combinations of enzymes, that is, each curve represents the DNA repair within a given spore from the spore population. The horizontal axis represents the repair time in seconds. The vertical axis is split between the fraction of remaining DNA after an exposure time of 2 seconds at a temperature of 300°C , $f_D(T, t_e)$, and the fraction of damaged DNA repaired, ξ_5. Approximately 76 % of the DNA is still viable based on the notional values given in Table 4.1, 5.1 and 5.2. The red dashed line represents a critical threshold for DNA set to 95% of total DNA, ξ_c=.95. If all of the curves lie below this critical threshold at an arbitrary chosen outgrowth time, t_0=*150* seconds, then the spore's probability of survival is zero. However, if the outgrowth time is chosen to be larger, say t_0=*250* seconds, then some of the curves lie above this critical threshold while others lie below. This will lead to a nonzero probability of survival for the spore.

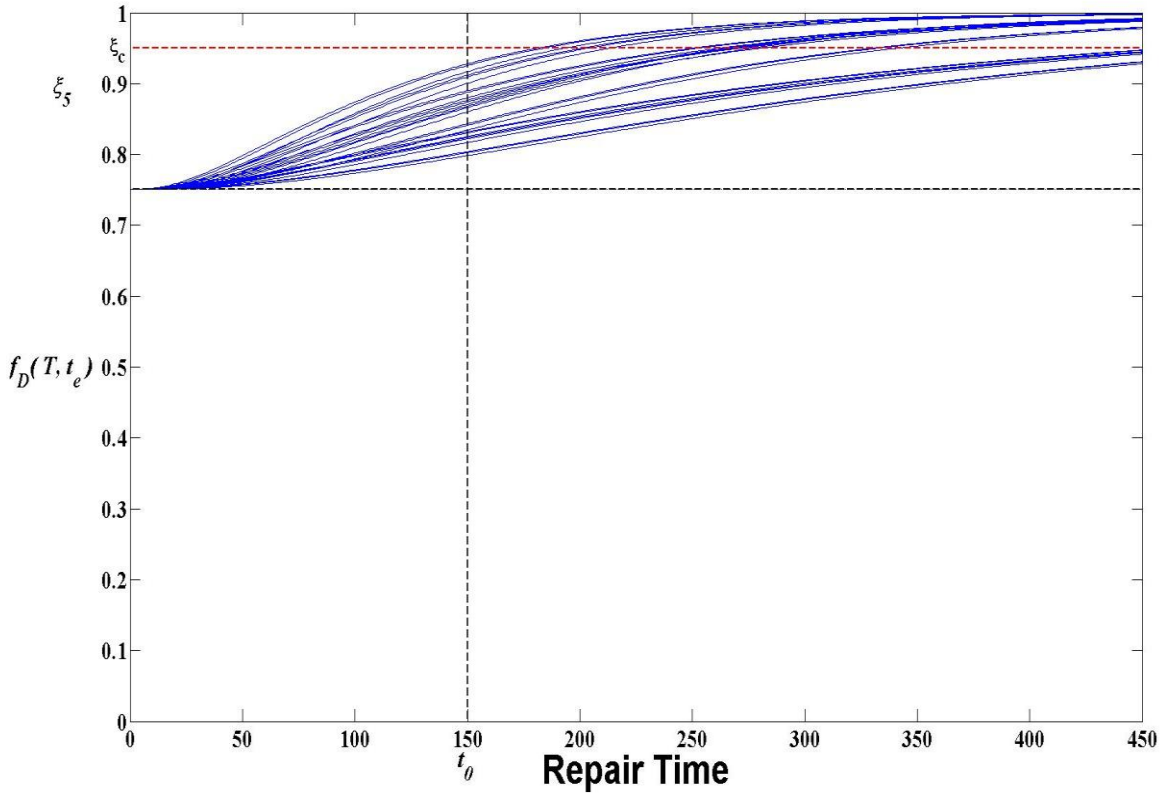

Figure 5.10: Critical DNA Threshold

The distribution of curves depicted in Figure 5.10 is dependent on the distribution of enzymes. As mentioned before, the combinations of viable enzymes will influence the DNA repair process. To further explore this influence, consider different enzyme combinations that satisfy

$$\xi_5(t_r,\gamma)+f_D(T,t_e)=\xi_c \tag{5.23}$$

Using the nonlinear model from Equation 5.16 with fixed exposure time, exposure temperature, and outgrowth time, while each enzyme varied between zero and one, it was observed that different enzyme combinations effected the percentage of damaged DNA that is repaired, ξ_5.

Figure 5.11 illustrates the different combinations of enzymes that will yield particular threshold values as given in Equation 5.23. The blue surface represents the different sets of enzymes when $\xi_c = .85$. The green surface represents the combination of enzymes when $\xi_c = .90$ and the red surface represents those when $\xi_c = .95$. The domain of integration for the probability of kill would include all combinations of enzymes below their respective critical surface. For example, the domain of integration for the probability of kill when the critical threshold is .95 would include all combinations of enzymes below the red surface moving toward the origin.

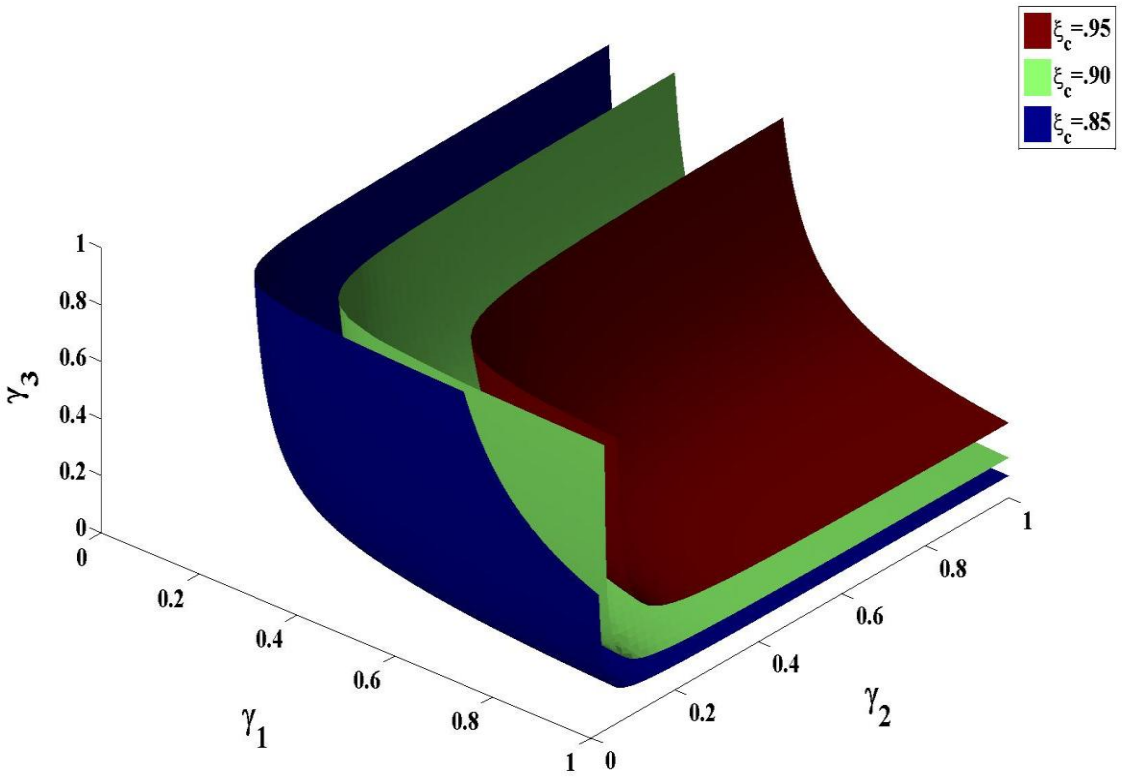

Figure 5.11: Enzyme Combinations for Different Critical Thresholds

Based on I_0=100 nM, t_e = 2 sec, T = 350°C, α=10, β=3, t_o = 250 sec, and values from Table 5.1 and 5.2.

After have defining the probability of kill and the domain of integration, calculations can be made to determine how outgrowth time influences the spore's probability of survival after a fixed exposure temperature and time.

5.5.3 Probability of Survival Calculations.

Outgrowth time is a key factor for the spore's probability of survival. For example, after 2 minutes there might not be any visible vegetative cells formed from the spores. After 20 minutes there might be several visible vegetative cells. This is because the spore has more time to repair damaged DNA. Therefore, in order to look at the spore's chance of survival, the probability of survival will be computed for three different outgrowth times as well as for two different fixed exposure temperature and time.

The probability of survival, P_s, is defined as

$$P_s = 1 - P_k(\xi_5(t_r, \gamma) + f_D(T, t_e) < \xi_c).$$

Table 5.4 gives the probability of survivals for different outgrowth times. These calculations were based on t_e = 2 seconds, T = 300°C, I_0 = 100 nM, $\alpha = 10$, $\beta = 3$, ξ_c = .95 and the values from Tables 5.1 and 5.2.

Table 5.4: Probability of Survival for Different Outgrowth Times (300°C 2 sec)

Outgrowth Times	**Probability of Survival**
120 seconds	0 %
240 seconds	58 %
300 seconds	94 %

From Table 5.4, as the outgrowth time increase, the spore's chance of survival also increases. Increased outgrowth time gives the spore additional time to repair damaged DNA as expected. Therefore, if the spore's enzymes are substantially damaged, the longer outgrowth time is crucial for the repair process since the rate velocities will be slow.

Table 5.5: Probability of Survival for Different Outgrowth Times (400^{o}C .01 sec)

Outgrowth Times	**Probability of Survival**
300 seconds	0 %
540 seconds	41 %
720 seconds	94 %

Table 5.5 gives the probability of survivals for different outgrowth times. These calculations were based on t_e = .01 second, T = 400^{o}C, I_0 = 100 nM, $\alpha = 10$, $\beta = 3$, ξ_c = .95 and the values from Tables 5.1 and 5.2. The increase in temperature allows pyrolysis reactions to occur. Therefore, the longer outgrowth times are required for higher probability of survival.

6. Conclusions and Future Work

6.1 Conclusions

In Chapter 3, the thermogravimetric analysis data obtained from Dr. Felker [18] was examined. The purpose of this data was to estimate the water content within the spore and the temperatures at which this water would become mobile. From these results it was concluded that the absorbed water becomes mobile around a peak of 105^{o}C and the chemically bound water becomes available for release at a peak of 290^{o}C. These findings verify the assumptions made previously [19] who assumed that the absorbed water is released at a peak of 100^{o}C and chemically bound water is released at a peak of 300^{o}C. Additionally, the spore's weight was estimated to be about 40-45% water. The amount of water within the spore is important for hydrolysis reactions to occur.

Chapter 4 examined the type of damage occurring within the spore. Damage can be caused by hydrolysis and pyrolysis reactions. The hydrolysis reactions can cause damage to the spore's DNA and enzymes. This damage includes deamination, depurination, denaturation, and depolymerization. Furthermore, five different DNA repair mechanisms within the spore were discussed with emphasis on BER as the repair mechanism responsible for spore outgrowth. It was assumed that a spore taken from a spore population begins with 100% healthy DNA information and that the DNA information diminishes exponentially based on rate coefficients corresponding to hydrolysis and pyrolysis reactions. Following this further, the initial fitness distribution of enzymes developed by Captain Knight which followed a Gaussian distribution was

enhanced by using a scaled beta distribution that corrects the concentration of enzymes within the spore to fall between zero and some maximum value. Using both the Gaussian and scaled beta distributions, probability of survival models were developed to examine the spore's chance of survival. These probability of survival models were based on knowledge of a critical enzyme threshold, that is, the value below which the spore does not contain the sufficient concentration of enzymes for the DNA repair process. Using the notational values, it was concluded that when heating the spore population at a temperature of 225^{o}C during dry heating and a threshold of 0.10, the probability of survival was estimated to drop off faster when using the beta representation. This is because the Gaussian distribution was not bounded above as was the beta distribution. However, because the enzyme critical threshold is unknown and the model is compared to actual data collected after outgrowth, there is a need for an outgrowth model.

The spore will break dormancy once placed in a nutrient rich environment. Once this begins, the spore moves into germination. Germination occurs when the spore's metabolic activity resumes and the spore begins repairing the damaged DNA. It was asserted that the BER mechanisms will be necessary to repair the damaged DNA. This assertion was based on the type of damage caused within the spore from hydrolysis reactions. Quantitative models exist for this DNA repair process within humans. Since these repair process are conserved from bacteria to humans, these models were mimicked to provide a qualitative understanding of the process within the spore. Since the focus was on DNA information content instead of concentration, a dimensionless variable, $y_i = \xi I_0$ was introduced as was the initial state of DNA within the repair model. The

initial state of DNA plays a major role in the nonlinear DNA BER model. It was concluded that if $\xi_i I_0 << K_i$, then the DNA BER model could be linearized and an analytical solution was found. Also, by using the linear model, the exposure time influence was shown to appear only in the exponential terms. This means that the exposure time will only change the rate at which the repair velocity equilibrates. When $\xi_i I_0 \approx K_i$, then the DNA BER model must remain nonlinear and a numerical method must be used to find the solution. Additionally, since the concentration of enzyme's initial distribution was based on a beta distribution, additional assumptions were made about the maximum concentration for each type of enzyme present during the repair process. If the spore's DNA is repaired, the spore then moves into the last stage which is outgrowth. The time at which survival is assessed plays a crucial role in the determination of the spore's survival. Using this fact and the enzyme influence on the repair process, a probability of survival model was developed. Unlike before, this model is not based on critical threshold values for the enzymes. Instead, the probability of survival model is based on a threshold value for the DNA information. Since the enzymes as well as the DNA are damaged during the thermal inactivation, they influence the DNA repair process which in turn influences the probability of survival. Using the probability of kill model with the notational values, it was concluded that with a fix exposure time of 2 seconds, a temperature of 300^{o}C, and an initial state of DNA, $I_0 = 100\ nM$, if given an outgrowth time of 120 seconds, the spore has a 0 % chance of survival. With an outgrowth time of 240 seconds, the spore's chance of survival increases to 58 % and with an outgrowth time of 300 seconds, the spore's chance of survival increase to 94 %.

6.2 Future Work

The Gaussian and beta distributions were looked at for the initial enzyme distribution. However, additional distributions could be considered. The DNA BER model was based on human DNA and even though, there is comparison between bacteria and human DNA repair process, possible refinement in the model should be considered for future work. Moreover, to execute the model, kinetics data found in literature based on human DNA was used. It would be advisable to compare the model to actual experimental data from the spore. In addition, when developing the probability of survival model in Chapter 5 only the nonlinear model was considered. The linear model might provide additional insight into the spore's chance of survival. Further, assumptions about independence for the enzymes were made. This assumption may not hold true, therefore a joint distribution will need to be consider. Lastly, this research only considered hydrolysis reactions within the spore. Additional work should be done that looks at the affects of the physical and chemical environment on the spore. Along with various chemical and biologic processes that can affect the probability of survival of a *B.a* spore after heat treatment.

Bibliography

1. Berg, Jeremy M., John L. Tymoczko, and Lubert Stryer. *Biochemistry* (6th Edition). New York: W.H. Freeman & Company, 2007.

2. Coates, Philip J., Sally A. Lorimore, and Eric G. Wright. "Cell and Tissue Responses to Genotoxic Stress," *Journal of Pathology*, 205: 221-235 (2005).

3. Cooper, Geoffrey M. and Robert E. Hausman. *The Cell: A Molecular Approach* (5th Edition). Washington D.C.: ASM Press, 2009.

4. Dixon, Terry C., Matthew Meselson, Jeanne Guillemin, and Philip C. Hanna. "Anthrax," *The New England Journal of Medicine*, 341: 815-826 (1999)

5. Doughty, Alan and John C. Mackie. "Kinetics of Thermal Decomposition of the Diazines: Shock-tube Pyrolysis of Pyrimidine," *Journal of the Chemical Society, Faraday Transactions,* 90: 541-548 (1994).

6. Driks, Adam. "The *Bacillus subtilis* spore coat," *Microbiology and Molecular Biology Reviews*, 63: 1-20 (March 1999).

7. Driks, Adam. "The Dynamic Spore." *PNAS*, 100: 3007-3009 (March 2003).

8. Fleck, Oliver and Olaf Nielsen. "DNA repair," *Journal of Cell Science*, 117: 515-517 (2004).

9. "Endospore." 10 February 2011 <http:// wapedia.mobi/en/Endospore>.

10. Felker, Daniel. Analytical Chemist, AFIT, Personal Correspondence. 30 November 2010.

11. Gerhardt, P.C. and R. E. Marquis. "Spore Thermoresistance Mechanisms," *Regulation of Prokaryotic Development,* Washington DC: American Society for Microbiology, (1989).

12. Giri, Narayan C. *Introduction to Probability & Statistics* (2nd Edition). New York: Marcel Dekker Inc., 1993.

13. Goetz, Kristina M. *Lethality of Bacillus Anthracis Spores Due to Short Duration Heating Measured Using Infrared Spectroscopy.* MS thesis, AFIT/GNE/ENP/05-04. Graduate School of Engineering and Management, Air Force Institute of Technology (AU), Wright-Patterson AFB OH, March 2005.

14. Gould, G.W. "Recent Advances in the Understanding of Resistance and Dormancy in Bacterial Spores," *Journal of Applied Bacteriology*, 42: 297-309 (1977).

15. Gradshteyn, I.S. and I. M. Ryzhik. *Table of Integrals, Series, and Products* (4th Edition). New York & London: Academic Press, 1965.

16. Hawkins, Leslie S. *Micro-Etched Platforms for Thermal Inactivation of Bacillus Anthracis and Bacillus Thuringiensis Spores*. MS thesis, AFIT/GWM/ENP/08-M01. Graduate School of Engineering and Management, Air Force Institute of Technology (AU), Wright-Patterson AFB OH, March 2008.

17. Hansen, J.N., G. Spiegelman, and H.O. Halvorson. "Bacterial Spore Outgrowth: Its Regulation," *Science*, 168: 1291-1298 (1970).

18. Inglesby, Thomas V. and others. "Anthrax as a Biological Weapon," *JAMA*, 281: 1735-1745 (1999).

19. Knight, Emily A. *Modeling Thermal Inactivation of Bacillus Spores*. MS thesis, AFIT/GAM/ENC/09-01. Graduate School of Engineering and Management, Air Force Institute of Technology (AU), Wright-Patterson AFB OH, March 2009

20. Kobayashi, Y., W. Steinberg, A. Higa, H. O. Halvorson, and C. Levinthal. "Sequential Synthesis of Macromolecules during Outgrowth of Bacterial Spores," In L.L Campbell, and H. O. Halvorson (ed), Spores III. *American Society for Microbiology*, Ann Arbor, Mich. p. 200-212.

21. Leuschner, Renata G.K. and Peter J. Lillford. "Investigation of Bacterial Spore Structure by High Resolution Solid-State Nuclear Magnetic Resonance Spectroscopy and Transmission Electron Microscopy," *International Journal of Food Microbiology*, 35: 35-50 (2001).

22. Lindahl, Tomas and Barbro Nyberg. "Heat-Induced Deamination of Cytosine Residues in Deoxyribonucleic Acid," *Biochemistry*, 13: 3405-3410 (1974).

23. Melly, E., P. C. Genest, M.E. Gilmore, S. Little, D. L. Popham, A. Driks, and P. Setlow. "Analysis of the properties of spores of Bacillus subtilis prepared at different temperatures," *Journal of Applied Microbiology*, 92:1105-1115 (2000).

24. Menczel, Joseph D. and R. Bruce Prime. *Thermal Analysis of Polymers, Fundamentals and Applications*. Hoboken, New Jersey: John Wiley & Sons, Inc., 2009.

25. Meot-Ner (Mautner), Michael, Ashok R. Dongre, Arpad Somogyi, and Vicki H. Wysocki. "Thermal Decomposition Kinetics of Protonated Peptides and Peptide Dimers, and Comparison with Surface-induced Dissociation," *Rapid Communications in Mass Spectrometry*, 9: 829-836 (1995).

26. Missiakas, Dominique M. and Olaf Schneewind. "*Bacillus anthracis* and the Pathogenesis of Anthrax," In Luther E. Lindler, Frank J. Lebeda, and George W. Korch (ed), Biological Weapons Defense: Infectious Diseases and Counterterrorism. *Infectious Diseases*, Totowa, NJ. p. 79-97.

27. Moberly, Betty J., F. Shafa, and Philipp Gerhardt. "Structural Details of Anthrax Spores During Stages of Transformation into Vegetative Cells." *Journal of Bacteriology*, 92: 220-228 (1966).

28. Mohomed, Kadine. "Thermogravimetric Analysis Theory, Operation, Calibration and Data Interpretation." 18 August 2010 < http://membrane.ces.utexas.edu/Home/LabPractice/TGA.ppt>.

29. Mohr, Peter J. and Barry N. Taylor. "CODATA Recommended Values of the Fundamental Physical Constants: 2006," *Review of Modern Physics*, 80: 633-730 (December 2007).

30. Plomp, Marco, Terrance J. Leighton, Katherine E. Wheeler, Haley D. Hill, and Alexander J. Malkin. "In vitro high-resolution structural dynamics of single germinating bacterial spores". *PNAS*, 104: 9644-9649 (2007).

31. Rubinow, S.I. *Introduction to Mathematical Biology*. New York: John Wiley & Sons, Inc., 1975.

32. Schwarzenbach, Rene P. *Environmental Organic Chemistry*. New York: John Wiley & Sons, Inc., 1993.

33. Setlow, Peter. "The Bacterial Spore: Nature's Survival Package." *Culture*, 26: 1-4 (September 2005).

34. Setlow, Peter. "Spores of *Bacillus subtilis*: Their Resistance To and Killing by Radiation, Heat and Chemicals." *Journal of Applied Microbiology*, 101: 514-525 (2006).

35. Setlow, Peter. "I Will Survive: Protecting and Repairing Spore DNA." *Journal of Bacteriology*, 174: 2737-2741 (May 1992).

36. Sokhansanj, Bahrad A., Garry R. Rodrigue, J. Patrick Fitch, and David M. Wilson III. "A Quantitative Model of Human DNA Base Excision Repair. I. Mechanistic Insights," *Nucleic Acids Research*, 30: 1817-1825 (2002).

37. Tainer, John A., Maria M. Thayer, and Richard P. Cunningham. "DNA Repair Proteins," *Current Opinion in Structural Biology*, 5: 20-26 (1995).

38. "Thermogravimetric Analysis (TGA)/ Differential Thermal Analysis (DTA)." 18 August 2010 <http://www.cea.com/techniques/analytical_techniques/tga_dta.php>.

39. Willet, Hilda P. and Suydam Osterhout. “Bacillus,” In Joklik, Wolfgang K. and Hilda P. Willett (ed), Zinsser Microbiology. New York: Appleton-Century-Crofts, 1976.

40. Yoshii, H., Furuta, T., Noma, S., and Noda, T. “Kinetic Analysis of Soy-protein Denaturation by a Temperature Programmed Heat-denaturation Technique,” *Agricultural and Biological Chemistry*, 54: 863-869 (1990).

REPORT DOCUMENTATION PAGE

Form Approved
OMB No. 074-0188

PLEASE DO NOT RETURN YOUR FORM TO THE ABOVE ADDRESS.

1. REPORT DATE *(DD-MM-YYYY)*	2. REPORT TYPE	3. DATES COVERED *(From – To)*
24-03-2011	Master's Thesis	September 2009 – March 2011

TITLE AND SUBTITLE

Modeling of *Bacillus* spores: Inactivation and Outgrowth

5a. CONTRACT NUMBER

5b. GRANT NUMBER

5c. PROGRAM ELEMENT NUMBER

6. AUTHOR(S)

Hurst, Alexis X.

5d. PROJECT NUMBER
JON: 10P281 JON: 11P113

5e. TASK NUMBER

5f. WORK UNIT NUMBER

7. PERFORMING ORGANIZATION NAMES(S) AND ADDRESS(S)
Air Force Institute of Technology
Graduate School of Engineering and Management (AFIT/ENC)
2950 Hobson Way, Building 641
WPAFB OH 45433-8865

8. PERFORMING ORGANIZATION REPORT NUMBER

AFIT/GAM/ENC/11-01

9. SPONSORING/MONITORING AGENCY NAME(S) AND ADDRESS(ES)
AFNWC/EN Attn: Lt. Col Brian L. Evans and Ms. Angelica I. Rubio
1551 Wyoming Blvd SE, Kirtland AFB, NM 87117 (505)853-3266

Defense Threat Reduction Agency Attn: Su Peiris, RD-BAS, Cube 3645E
8725 John J Kingman Rd STOP 6201, Fort Belvoir, VA 22060-6201

10. SPONSOR/MONITOR'S ACRONYM(S)
AFNWC/EN DTRA

11. SPONSOR/MONITOR'S REPORT NUMBER(S)

12. DISTRIBUTION/AVAILABILITY STATEMENT

APPROVED FOR PUBLIC RELEASE; DISTRIBUTION UNLIMITED.

13. SUPPLEMENTARY NOTES

14. ABSTRACT This research models and analyzes the thermochemical damage produced in *Bacillus* spores by short, high-temperature exposures as well the repair process within damaged *Bacillus* spores. Thermochemical damage in spores is significantly due to reaction with water, hydrolysis reactions. Applying heat to the spore causes absorbed and chemically bound water molecules become mobile within the spore. These mobile water molecules react by hydrolysis reactions to degrade DNA and enzyme molecules in the spore. In order to survive the thermal inactivation, the spore must repair the damaged DNA during spore germination. The DNA repair process, as well as other germination functions, is dependent on reactions catalyzed by enzymes that are viable after the thermal exposure. Increased damage to the enzymes during thermal inactivation, affects the rate at which the spore DNA is repaired. If the enzymes are damaged to such an extent that the DNA repair is not completed, the spore is unable to germinate, or produce outgrowth. The DNA repair process, repair enzymes, and outgrowth time influences the spore's chance of survival. Using this information, a probability of survival model was created based on water mobility, hydrolysis reactions, an initial state of DNA, viable repair enzymes, and an outgrowth time.

15. SUBJECT TERMS
Bacillus, anthrax, thermal exposure, DNA repair, outgrowth

16. SECURITY CLASSIFICATION OF:			17. LIMITATION OF ABSTRACT	18. NUMBER OF PAGES	19a. NAME OF RESPONSIBLE PERSON
a. REPORT	b. ABSTRACT	c. THIS PAGE			William P. Baker, PhD (ENC)
U	U	U	UU	98	19b. TELEPHONE NUMBER *(Include area code)* (937) 255-6565, x4517 william.baker@afit.edu

Standard Form 298 (Rev. 8-98)
Prescribed by ANSI Std. Z39-18